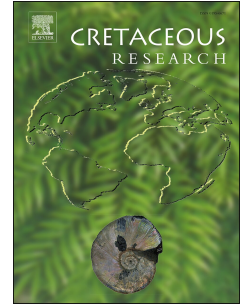


# Journal Pre-proof

A second specimen of the pterosaur *Thapunngaka shawi* from the Lower Cretaceous (upper Albian) Toolebuc Formation of North West Queensland, Australia

Timothy M. Richards, Paul E. Stumkat, Steven W. Salisbury



PII: S0195-6671(23)00268-9

DOI: <https://doi.org/10.1016/j.cretres.2023.105740>

Reference: YCRES 105740

To appear in: *Cretaceous Research*

Received Date: 10 July 2023

Revised Date: 29 September 2023

Accepted Date: 3 October 2023

Please cite this article as: Richards, T.M., Stumkat, P.E., Salisbury, S.W., A second specimen of the pterosaur *Thapunngaka shawi* from the Lower Cretaceous (upper Albian) Toolebuc Formation of North West Queensland, Australia, *Cretaceous Research*, <https://doi.org/10.1016/j.cretres.2023.105740>.

This is a PDF file of an article that has undergone enhancements after acceptance, such as the addition of a cover page and metadata, and formatting for readability, but it is not yet the definitive version of record. This version will undergo additional copyediting, typesetting and review before it is published in its final form, but we are providing this version to give early visibility of the article. Please note that, during the production process, errors may be discovered which could affect the content, and all legal disclaimers that apply to the journal pertain.

© 2023 The Author(s). Published by Elsevier Ltd.

1 A second specimen of the pterosaur *Thapunngaka shawi* from the Lower Cretaceous (upper  
2 Albian) Toolebuc Formation of North West Queensland, Australia

3 TIMOTHY M. RICHARDS <sup>1\*</sup>, PAUL E. STUMKAT <sup>2</sup> and STEVEN W. SALISBURY <sup>1</sup>

4 <sup>1</sup>School of the Environment, The University of Queensland, St. Lucia, Queensland, 4072,  
5 Australia; e-mails: [timothy.richards@uq.edu.au](mailto:timothy.richards@uq.edu.au), [s.salisbury@uq.edu.au](mailto:s.salisbury@uq.edu.au)

6 <sup>2</sup>P.O. BOX 165, Killarney, Queensland, 4373, Australia; e-mail:  
7 [paul@stumkatstudios.com.au](mailto:paul@stumkatstudios.com.au)

8 \*Corresponding author

9

10

11

12

13

14

15

16

17

18

19

20

**21 Abstract.**

22 Herein, we describe a second specimen of *Thapunngaka shawi*, a large pterosaur from the  
23 Lower Cretaceous (upper Albian) Toolebuc Formation of North West Queensland, Australia.  
24 The new specimen (KKF600) consists of the anteriormost portion of an incomplete  
25 premaxillary/maxillary rostrum embedded in matrix and a caudal fragment preserving a left  
26 portion of the maxillary rostrum. KKF600 shares with the holotype (KKF494) near identical  
27 features pertaining to alveolar morphology and patterning, and complementary similarities  
28 between the palatal and dentary occlusal surfaces, respectively. Subsequently, we present a  
29 revised diagnosis of *Thapunngaka shawi*. A phylogenetic analysis recovers a clade formed by  
30 the genera *Thapunngaka*, *Ferrodraco* and *Mythunga*. The recognition of this pterosaur clade,  
31 Mythungini, points to a possible East Gondwanan radiation within Tropeognathinae.

**32 Keywords**

33 *Thapunngaka shawi*, Mythungini, Toolebuc Formation, Pterodactyloidea, Cretaceous

**34 1. Introduction**

35 The pterosaur fossil record is vast, spanning roughly 150 million years from the Upper  
36 Triassic through to the end of the Cretaceous (Unwin, 2006). Achieving an essentially global  
37 distribution throughout this time, pterosaur remains have been found on every continent  
38 (Barrett et al., 2008, Kellner et al., 2019). The vast majority of pterosaur remains derive from  
39 Lagerstätten such as the Solnhofen Limestone of Germany, the Santana and Crato formations  
40 of Brazil, the Niobrara Chalk of North America and the Yixian and Jehol formations of China  
41 (Witton, 2013). These unique sites, often yielding near complete specimens, some with  
42 associated soft tissue, have undoubtedly improved our knowledge of these otherwise  
43 enigmatic animals (e.g., Kellner and Tomida, 2000, Bennett, 2002, Xiaolin and Zhonghe,  
44 2006). However, localities such as these are rare and are separated by enormous temporal and

45 geographic distances. Moreover, with the exception of these few sites, the rest of the world's  
46 pterosaur record is relatively poor, represented by fragmentary and often isolated material. As  
47 such, our true understanding of pterosaur diversity and their evolutionary history remains  
48 somewhat limited (Butler et al., 2013, Jacobs et al., 2019). This is particularly true for  
49 Australia.

50 By any standard, the Australian pterosaur fossil record is modest, surpassing only Antarctica  
51 in terms of taxonomic diversity and specimens described; however, it is improving. Recent  
52 discoveries from the Cretaceous Rolling Downs Group of western Queensland have doubled  
53 the number of species of named Australian pterosaurs (from two to four) and increased our  
54 understanding of Australian pterosaur diversity. Following the recent pterosaur phylogeny  
55 proposed by Holgado and Pêgas (2020) there are currently three recognised Australian  
56 anhanguerids: *Mythunga camara* (QMF18896) (Molnar and Thulborn, 2007); *Thapunngaka*  
57 *shawi* (KKF494) (Richards et al., 2021); and *Ferrodraco lentoni* (AODF876) (Pentland et al.,  
58 2019). *Mythunga camara* and *Thap. shawi* are both from the upper Albian Toolebuc  
59 Formation of North West Queensland, while *F. lentoni* derives from the younger  
60 (Cenomanian–lower Turonian) upper Winton Formation. By contrast, *Aussiedraco molnari*  
61 (QMF10613) (Kellner et al., 2011), also from the Toolebuc Formation, is the only recognised  
62 non-anhanguerian Australian species, being recently assigned to the Targaryendraconidae by  
63 Pêgas et al. (2019). In addition to the named species, the ctenochasmatoïd humeral fragment  
64 (QMF42739) (Fletcher and Salisbury, 2010) from the upper Albian Mackunda Formation of  
65 North West Queensland and the putative azhdarchid ulna (WAM 60.57) (Bennett and Long,  
66 1991) from the upper Maastrichtian Miria Formation of Western Australia most likely  
67 represent distinct non-anhanguerian taxa. Furthermore, a jaw fragment (WAM 68.5.11) (Kear  
68 et al., 2010) from the Cenomanian Molecap Greensand of Gingin, north of Perth, south-  
69 western Western Australia, also possibly represents a distinct anhanguerian taxon. It is

70 therefore reasonable to assume that at least seven pterosaur taxa, representing four distinct  
71 pterodactyloid clades (Anhangueridae, Targaryendraconidae, Ctenochasmatidae and  
72 Azhdarchidae) were present in Australia during the Cretaceous.

73 Concerning the phylogenetic relationships of *M. camara*, *F. lentoni* and *Thap. shawi*, recent  
74 analyses have consistently supported their close relationship within Anhangueridae. Pentland  
75 *et al.* (2019, fig. 7A), using the modified dataset of Andres *et al.* (2014), recovered *M.*  
76 *camara* and *F. lentoni* in a sister-group relationship within Anhangueria with *Ornithocheirus*  
77 *simus*, *Coloborhynchus clavirostris* and *Tropeognathus mesembrinus* as their successive  
78 sister-taxa. Using an entirely different dataset, Holgado and Pêgas (2020, fig. 10) also  
79 recovered the same sister-group relationship between the two Australian taxa. However, the  
80 latter analysis differed from the former in that it recovered *Trop. mesembrinus* and  
81 *Siroccoptyx moroccensis* as their successive sister-taxa to the Australian clade. Holgado  
82 and Pêgas (2020) subsequently assigned of all four taxa to a new clade called  
83 Tropeognathinae. Notably, neither *C. clavirostris* nor *O. simus* were recovered as members of  
84 Tropeognathinae; the former was found to be a basal coloborhynchine, the latter a basal  
85 ornithocheiraeon (see Holgado *et al.* 2019 and Holgado and Pêgas 2020 for a detailed  
86 discussion). Most recently, Richards *et al.* (2021, fig. 4) included the newly recognised  
87 anhanguerid *Thap. shawi* in two phylogenetic analyses, using both the Holgado and Pêgas  
88 (2020) and Andres *et al.* (2014) datasets. Interestingly, despite being based different datasets,  
89 both analyses recovered all three Australian taxa in an unresolved clade within Anhangueria.  
90 In each of the aforementioned analyses, recovery of this clade is based on the presence of one  
91 shared feature: robust and strongly raised alveoli borders.

92 In the present study, we describe new material comprising an incomplete maxillary rostrum  
93 of a large pterosaur from the Lower Cretaceous (upper Albian) Toolebuc Formation of  
94 Richmond, North West Queensland. The material (KKF0600) includes two pieces of the

95 rostral portion of a large crested rostrum. This is the thirteenth pterosaur specimen to be  
96 described from the Toolebuc Formation. Its description allows for a detailed reassessment of  
97 the phylogenetic relationships of Australian Cretaceous pterosaurs.

98

## 99 **2. Locality and Geological Setting**

100 The new specimen, KKF0600, was discovered by Ian Bool in June 2011 on Wunumara  
101 Country in a locality historically known as ‘Cambridge Quarry’, which is located on  
102 Morungle Station, a large pastoral property covering approximately 242 square kilometres  
103 (24,200 hectares). The quarry is located a few hundred metres off the Richmond-Woolgar  
104 Road, about 40 km northwest of the township of Richmond, North West Queensland,  
105 Australia (Fig. 1). Past excavations of this quarry have exposed a sequence of heavily  
106 weathered, laminated mudstone, typical of the Toolebuc Formation. Throughout the quarry  
107 the exposed sequence ranges in thickness from 1–6 metres. The specimen described herein  
108 was found in a low lying and heavily eroded area of the quarry where the mudstone is  
109 approximately 1.5 m thick (Fig. 2).

110 Conformably overlain by the Allaru Mudstone and overlying the Wallumbilla Formation, the  
111 Toolebuc Formation forms part of the Rolling Downs Group (upper Aptian–lower Turonian),  
112 a continuous sequence of strata deposited within the Eromanga Basin. It records a period of  
113 extensive marine inundation covering more than 60 per cent of the continent (Campbell and  
114 Haig, 1999, Tucker et al., 2013) (Fig. 2). With an average thickness of 15 metres (Senior et  
115 al., 1975, Exon and Senior, 1976, Jiang et al., 2018), the Toolebuc Formation is a thin  
116 isochronous unit, considerably thinner than other units of the Rolling Downs Group and  
117 represents maximum flooding marine conditions within an epeiric basin (Campbell and Haig,

118 1999, Jell, 2013). It is easily recognized on the basis of a strong gamma-ray anomaly in  
119 wireline-logs (Exon and Senior, 1976).

120 The Toolebuc Formation is predominately mudstone, consisting of organic-rich shales. Thin  
121 beds of siltstone, sandstone and coquinitic and nodular limestones are also interspersed  
122 within the unit (Gray et al., 2002, McHenry, 2009, Jell, 2013). The mudstone contains  
123 extensive fish bone beds, colloquially known as ‘fish mash’. These beds consist of teeth,  
124 bones and scales from osteichthyian fish. Ammonites, belemnites, gastropods and bivalves  
125 are also found within the mudstone (Day, 1969, Exon and Senior, 1976, Henderson and  
126 Kennedy, 2002, McHenry, 2009). Indicative of a productive marine ecosystem, numerous  
127 teleost fishes have been described, including *Cooyoo australis* (Lees and Bartholomai, 1987),  
128 *Dugaldia emmilta* (Cavin and Berrell, 2019) and the predatory fishes *Richmondichthys sweeti*  
129 (Bartholomai, 2004) and *Australopachycormus hurleyi* (Kear, 2007a). Various sea turtles,  
130 including *Cratochelone berneyi* (Longman, 1915), *Bouliachelys suteri* (Kear, 2006) and the  
131 seemingly ubiquitous *Notochelone costata* (Owen, 1882) have also been reported. Marine  
132 tetrapods, including the endemic ichthyosaur *Platypterygius australis* (Zammit, 2010), the  
133 plesiosaur *Eromangasaurus australis* (Kear, 2007b) and the pliosaurid *Kronosaurus*  
134 *queenslandicus* (McHenry, 2009), are arguably the best known and most-documented fauna  
135 from the Toolebuc Formation.

136 Despite the marine depositional setting, several non-marine tetrapod fossils have also been  
137 discovered within the formation, including the ornithopod *Muttaborrasaurus* sp. (Molnar,  
138 1996), sauropods (Molnar, 1991, Molnar and Salisbury, 2005, Poropat et al., 2017), a  
139 thyreophoran dinosaur (Leahey and Salisbury, 2013), enantiornithine birds (Molnar, 1986,  
140 Kurochkin and Molnar, 1997) and several occurrences of pterosaurs (Molnar and Thulborn,  
141 1980, 2007, Molnar, 1987, Fletcher and Salisbury, 2010, Kellner et al., 2010, Kellner et al.,  
142 2011, Richards et al., 2021).

143 Based on palynological evidence, the Toolebuc Formation correlates with the *Coptospora*  
144 *paradoxa* and *Phimopolshawites pannosus* palynozones (Burger, 1982) and the lower part of  
145 the *Endoceratium ludbrookiae* dinocyst Zone (McMinn and Burger, 1986), indicative of an  
146 upper middle to lower upper Albian age (approximately 105–108 Mya). In conjunction with  
147 the spore-pollen assemblages, further support for this age is given by Bralower et al. (1993),  
148 who determined the Toolebuc Formation to contain the lowermost upper Albian  
149 *Axopodorhabus albianus* NC 9B nannofossil Zone.

### 150 **3. Materials and Methods**

#### 151 *3.1 Specimen*

152 KKF0600 (Figs. 3, 4) is housed at Kronosaurus Korner Regional Museum (an accredited  
153 Queensland State Government repository for significant natural history and cultural artifacts),  
154 in Richmond, North West Queensland, Australia. It was prepared by one of the authors,  
155 P.E.S., the then curator of Kronosaurus Korner Regional Museum, using mechanical methods  
156 only. Where necessary, cyanoacrylate and acetone-soluble acrylic resin (ethyl-methacrylate  
157 copolymer B72 paraloid) were used to seal the bone. A large fracture, extending through the  
158 entire slab immediately caudal to the 8<sup>th</sup> alveoli, has been repaired with epoxy glue.

#### 159 *3.2 Observations*

160 The specimen was examined by hand and measurements taken with digital calipers. A Nikon  
161 D5300 digital SLR camera was used for photography with Nikon 18–55 mm f/3.5–5.6 and  
162 Nikkor AF-S 40 mm f/2.8 DX micro lenses. The material was photographed under different  
163 lighting conditions including natural light and within a lighting box using warm-white LED  
164 lamps. For anatomical nomenclature and orientations, we follow Frey et al. (2003).

#### 165 *3.3 Phylogenetic analysis*

166 In order to assess the phylogenetic relationships of *Thapunngaka shawi* within Pterosauria, a  
167 phylogenetic analysis was performed using a modified version of the data matrix of Richards  
168 et al. (2021), which was, in turn, modified from the data matrix of Holgado and Pêgas (2020),  
169 containing 76 taxa and 179 discrete characters (Supplementary Data S1). Character scores for  
170 *M. camara*, *Aus. molnari* and *Thap. shawi* (including KKF494 and KKF0600) were obtained  
171 from first-hand study of the material. Character scores for all other taxa were taken from  
172 Holgado and Pêgas (2020), except scoring for *Amblydectes crassidens*, which was taken from  
173 Holgado (2021). All characters were unordered with *Ornithosuchus woodwardi*,  
174 *Herrerasaurus ischigualastensis* and *Scleromochlus taylori* used as outgroup taxa. The  
175 analysis was performed using the software TNT v1.5 (Goloboff and Catalano, 2016).  
176 Following the methodology of Holgado and Pêgas (2020), which was originally outlined in  
177 Pêgas et al. (2019), tree searches were conducted using Traditional Search (TBR swapping  
178 algorithm) utilising 10,000 replicates and random seed. Trees were collapsed after searching.  
179 A New Technology Search was also conducted via Sectorial Search with ratcheting  
180 (parameters: 20 substitutions, six up-weighting and six down-weighting probs., and 10  
181 iterations), tree fusing, Driven search (15 initial addseqs., 15 times minimum length), random  
182 seed without collapsing. To find the maximum number of minimum length trees, the results  
183 from the New Technology Search were then analysed via TBR using trees saved from RAM  
184 with no collapsing after search. Homoplasy indices: consistency index (CI), retention index  
185 (RI) and rescaled consistency index (RC) were calculated using the ‘Stats.run’ script  
186 available at the Willi Hennig Society website (<https://cladistics.org/tnt/>). Bootstrap values  
187 were calculated within TNT v1.5 using the ‘resampling’ function.

### 188 3.4 Institutional abbreviations

189 **AMNH**, American Museum of Natural History, New York; **AAOD**, Australian Age of  
190 Dinosaurs, Winton, Australia; **BSP**, Bayerische Staatssammlung für Paläontologie und

191 historische Geologie, Munich, Germany; **CAMSM**, Sedgwick Museum of Earth Sciences,  
192 Cambridge, England; **IVPP**, Institute of Vertebrate Paleontology and Paleoanthropology,  
193 Beijing, China; **IWCMS**, Isle of Wight County Museum Service, Isle of Wight, England;  
194 **KK**, Kronosaurus Korner, Richmond, Australia; **LINHM**, Long Island Natural History  
195 Museum, Levittown, New York, USA; **NHMUK**, Natural History Museum, London.  
196 England; **MHNS**, Museum of Natural History Sintra, Sintra, Portugal; **MN**, Museu  
197 Nacional/UFRJ, Rio de Janeiro, Brazil; **MPSC**, Museu de Paleontologia de Santana do  
198 Cariri, Santana do Cariri, Brazil; **MPZ**, Museo de Ciencias Naturales de la Universidad de  
199 Zaragoza, Zaragoza, Spain; **NSM**, National Science Museum, Tokyo, Japan; **QM**,  
200 Queensland Museum, Brisbane, Australia; **RGM**, National Natuurhistorisch  
201 Museum/Naturalis, Leiden, The Netherlands; **SAO**, Sammlung Oberli, St. Gallen,  
202 Switzerland; **SMNS**, Staatliches Museum für Naturkunde Stuttgart, Stuttgart, Germany;  
203 **SMU**, Shuler Museum of Paleontology, Southern Methodist University, Dallas, USA; **SNSB**,  
204 Staatliche Naturwissenschaftliche Sammlungen Bayerns-Bayerische Staatssammlung für  
205 Paläontologie und Geologie, Munich, Germany; **WAM**, Western Australia Museum, Perth,  
206 Australia.

## 207 **4. Results**

### 208 **4.1. Systematic Paleontology**

209 Pterosauria Kaup, 1834  
210 Pterodactyloidea Plieninger, 1901  
211 Ornithocheiroidea Seeley, 1870  
212 Lanceodontia Andres, Clark and Xu, 2014  
213 Anhangueria Rodrigues and Kellner, 2013  
214 Anhangueridae Campos and Kellner, 1985  
215 Tropeognathinae Holgado and Pêgas, 2020

216 **Mythungini** clade nov.

217 (Fig. 5)

218

219 *LSID*: zoobank.org:act:BEB61FD3-8C39-4728-8F0F-9092CA934995

220 *Type Genus*: *Mythunga* Molnar and Thulborn 2007.

221 *Stem-based definition*: The most inclusive clade containing *Mythunga camara* but not

222 *Tropeognathus mesembrinus*, *Amblydectes crassidens* nor *Sirocco moroccensis*.

223 *Taxa included*: *Mythunga camara* Molnar and Thulborn, 2007, *Thapunngaka shawi* Richards

224 et al., 2021, and *Ferrodraco lentoni* Pentland et al., 2019.

225 *Diagnosis*: Tropeognathine pterosaurs with strongly raised alveolar margins ('collars') on

226 both the upper and lower jaws.

227 *Remarks*: Here, we recognise Mythungini as a clade comprising *M. camara* (Albian,

228 Toolebuc Formation, Australia), *Thap. shawi* (Albian, Toolebuc Formation, Australia) and *F.*

229 *lentoni* (Cenomanian—Turonian, Winton Formation, Australia) within Tropeognathinae.

230 Previous phylogenetic analyses have consistently recovered a close relationship between

231 these taxa. Pentland et al. (2019), using the dataset of Andres et al. (2014), initially recovered

232 a sister-group relationship between *M. camara* and *F. lentoni* based on the presence of raised

233 alveolar borders. This relationship was corroborated by Holgado and Pêgas (2020) who

234 recovered them as sister-taxa within the clade Tropeognathinae along with *Trop.*

235 *mesembrinus* and *Siroccoptyx moroccensis* as consecutive sister taxa. Similarly, under the

236 two analyses of Richards et al. (2021), using the datasets of Holgado and Pêgas (2020) and

237 Andres et al. (2014), *Thap. shawi* was recovered as closely related to *M. camara* and *F.*

238 *lentoni*. In the present study, and each of the aforementioned analyses, all members of

239 Mythungini are united by the shared synapomorphy of raised alveolar borders.

240 *Occurrence:* Toolebuc Formation, Australia; Winton Formation, Australia; Albian–  
241 Cenomanian/Turonian (most likely Turonian).

242 *Thapunngaka shawi* Richards, Stumkat and Salisbury, 2021

243 *Revised Diagnosis:* Large tropeognathine pterodactyloid with the following apomorphies:  
244 dorsal surface of mandibular rostrum flat; occluding palatal surface of rostrum flat; third and  
245 sixth pair of alveoli largest in the maxillary and mandibular tooththrows, and subequal in size;  
246 dentary alveoli 6 through 13 positioned laterally on the mandible; alveoli 3 through 12  
247 positioned laterally on the maxillary rostrum; dentary and premax/max interalveolar distance  
248 increase gradually in size up to the sixth alveolus; large increase in interalveolar distance  
249 between seventh and eighth alveoli on both maxillary and mandibular rostrum (almost double  
250 the length of preceding interalveolar distance between sixth and seventh alveoli).

251 *Thapunngaka shawi* can be further distinguished from other anhanguerians by the following  
252 combination of characters: deep, ‘blade-like’ asymmetrical sagittal crest on the mandible with  
253 a gently concave rostral margin; mandibular and maxillary crests beginning at the rostral tip  
254 of the rostrum; very slight lateral expansion of the rostral part of the premax/maxillary and  
255 mandibular rostra; anteriormost portion of the maxillary and mandibular rostra directed  
256 dorsally when viewed laterally (beginning between the fourth and fifth alveoli).

257 *Holotype:* KKF494, the rostral portion of a mandible found on Wunumara Country,  
258 approximately 12 km northwest of Richmond, from the upper Albian Toolebuc Formation of  
259 North West Queensland, Australia.

260 *Referred specimen:* KKF0600, consisting of the rostral portion of an incomplete maxillary  
261 rostrum embedded in matrix (from the first to the eighth alveoli; Fig 3); and a caudal  
262 fragment preserving a caudal portion of the maxillary rostrum (with two alveoli, interpreted  
263 as the 11<sup>th</sup> and 12<sup>th</sup>; Figs. 3, 4). Measurements are given in Table 1.

264 *Locality:* Cambridge Quarry (20° 25' 34" S, 142° 56' 01" E), Wunumara Country,  
265 approximately 40 km northwest of Richmond, North West Queensland, Australia.

266 *Horizon:* Toolebuc Formation, Rolling Downs Group, Lower Cretaceous, upper Albian.

267 *Description of referred specimen, KKF600.*

268 *Preservation:* The larger piece (Fig 3) comprises a three dimensionally preserved incomplete  
269 premaxillary/maxillary rostrum. The left lateral side of the rostrum and part of the palatal  
270 surface are still partially embedded in a slab of carbonaceous mudstone that consists  
271 predominately of 'fish mash' (scales, bones and teeth), as is typical of certain horizons of the  
272 Toolebuc Formation from the Richmond area. The smaller fragment (Figs. 3, 4) is free from  
273 matrix and comprises a portion of the left maxilla, preserving two alveoli and the  
274 corresponding palatal surface. A broken crown is preserved in the caudal-most alveolus. In  
275 both pieces the cortical bone is light grey to reddish-brown, ranging in thickness from 0.6–1.5  
276 mm. Rostrally, the outer surface of the cortical bone is highly rugose, whilst the lateral  
277 surfaces are considerably smoother. However, most of the lateral surfaces have suffered  
278 considerable fracturing due to compaction caused by vertical over pressuring. There is no  
279 discernible suture between the fused premaxillae and the maxillae.

280 The rostrum is shallowly embedded in the slab to a level such that the entire right lateral side  
281 and most of the palatal and rostral surfaces are exposed. Comprising the rostral portion of the  
282 right premaxilla and maxilla, the specimen preserves the first eight alveoli on the right side.  
283 Due to the relief of the bone, the medial margin of the left sixth alveolus can also be seen.  
284 Based on this observation, and considering the labiolingual dimension of the respective  
285 alveolus on the right side, we estimate the entire rostrum is embedded to a depth of no greater  
286 than 6 or 7 mm.

287 The first right alveolus preserves a broken crown, the remaining alveoli do not preserve any  
288 teeth. Except for slight lateral crushing, all remaining alveoli are well preserved. The palatal  
289 surface is well preserved and undistorted, except for a section between the fourth and fifth  
290 alveoli which has suffered minor deformation from compaction.

291 The dorsal-most portion of the premaxillary crest is not preserved. However, impressions  
292 made by the left lateral side of the crest on the matrix reveals that the crest extended dorsally  
293 to at least the preserved margin of the slab (Fig. 3). Similar impressions are also observed on  
294 the caudal end of the slab rostral to alveoli eleven and twelve (Figs. 3 and 4).

295 The smaller fragment (Figs. 3 and 4) was found immediately next to the slab and is clearly  
296 associated with KKF0600, representing a more caudal portion of the left maxilla (see Fig.  
297 4E–F). The specimen comprises the relatively well-preserved lateral surface of the maxilla  
298 and corresponding palatal surface; the medial surface of the premax/maxilla has suffered  
299 considerable abrasion and is otherwise uninformative. Where preserved, the cortical bone is  
300 generally smooth with some minor fracturing. Two alveoli, considered to represent the left  
301 eleventh and twelfth left alveoli are also preserved. A broken crown is preserved in the  
302 twelfth alveolus. The preserved palatal surface of this fragment is smooth and undistorted.

303 *Osteology:* Specimen KKF0600 is the rostral portion of an incomplete rostrum, missing the  
304 dorsal margin of the premaxillary/maxillary crest. As preserved, the specimen is 312 mm  
305 long and the minimum height of the premaxillary crest is 82.8 mm, measured above the  
306 second alveolus. However, an impression made on the slab directly above the broken dorsal  
307 margin of the preserved crest represents a portion of left lateral surface of the premaxillary  
308 crest that is now missing (Fig. 3A-B). This impression measures approximately 140 mm  
309 rostrocaudally, and 19 mm dorsoventrally, demonstrating that the minimum height of the  
310 premaxillary crest was at least 102 mm. Multiple networks of small grooves and channels,

311 ranging in width from 0.5–1 mm, are visible on the right lateral surface of the premaxillary  
312 crest (Fig. 6). These features also occur on the impression left on the matrix (although  
313 represented by ridges). Similar features are not observed on any other part of the rostrum and  
314 may represent impressions of blood vessels associated with a rhamphotheca, resembling  
315 similar structures observed on the maxillary rostrum of other pterosaurs, such as  
316 *Thalassodromeus sethi*, *Tropeognathus* cf. *T. mesembrinus*, *M. camara* and *Dsungaripterus*  
317 *weii* (Kellner and Campos, 2002, Kellner et al., 2013, Pentland and Poropat, 2019, Chen et  
318 al., 2020).

319 In rostral view, the exposed outline of KKF0600 is subtriangular in shape (Fig. 3E–F), being  
320 much taller than wide. Immediately dorsal to the first alveolus, the right lateral margin  
321 gradually tapers dorsally for approximately 45 mm. Dorsal to this point, the width remains  
322 relatively uniform and thin (minimum width 4 mm). The rostralmost margin of the rostrum is  
323 rounded and highly rugose and extends dorsally for 39 mm from the palate at an angle of  
324 approximately 105°, meeting with the rostradorsal margin of the premaxillary crest. In lateral  
325 aspect, the rostradorsal margin of the premaxillary crest is slightly concave and extends  
326 caudodorsally at an angle of approximately 50° with respect to the rostralmost rostral margin.

327 In lateral aspect, the caudal portion (alveoli 5–12) of the palatal surface is straight. However,  
328 the rostral portion, beginning between the fourth and fifth alveoli, is deflected dorsally at an  
329 angle of approximately 15° relative to the plane defined by the caudal palatal surface. In  
330 ventral aspect, the exposed region of the palate is 9.5 mm wide at a point level with the fourth  
331 alveolus, narrowing to 7.6 mm at the fifth alveolus. Caudally, from alveoli five to eight, the  
332 width remains fairly constant. Rostral to the fourth alveolus, the palate expands slightly  
333 laterally, reaching a mediolateral width of 11.5 mm at the first alveolus. Despite a small  
334 amount of deformation near alveoli four and five, the palatal surface is smooth and there is no  
335 evidence of a median palatal ridge on either fragment of KKF0600 (Figs. 3C–D, 4B, D).

336 The specimen preserves the eight rostralmost right alveoli and the sixth (albeit partially),  
337 eleventh and twelfth left alveoli. All alveoli have a mesiodistally oval outline, although the  
338 fourth and sixth right alveoli are slightly more circular (Table 1). The first alveolus is located  
339 slightly caudal to the rostralmost margin of the rostrum and is directed rostroventrally, it also  
340 contains the root of a broken premaxillary tooth and a small amount of matrix. The second  
341 through to the fifth right alveoli are situated more lateroventrally on the rostrum. Caudally,  
342 the sixth, seventh and eighth right alveoli and the eleventh and twelfth left alveoli are  
343 positioned almost laterally on the maxilla. Except for the first and second right alveoli, all  
344 alveoli are surrounded by robust bony collars measuring 2-3 mm in thickness. The lateral  
345 margins of the maxilla are deeply scalloped and sulcate between each alveolus. A well-  
346 pronounced groove, located between the fourth and fifth right alveoli, measuring 3.3 mm in  
347 depth mediolaterally and 15 mm in length dorsoventrally, is tentatively interpreted as an  
348 occlusal groove for the fourth mandibular tooth.

349 The broken crown preserved in the twelfth left alveolus is slightly labiolingually compressed  
350 with an oval basal cross-section and is directed lateroventrally. Due to poor preservation, any  
351 enamel ornamentation (such as longitudinal grooves or carinae) that may have been present,  
352 is not visible. Despite missing the apical end, it is clear the tooth was likely elongated  
353 basiapically and conically shaped, as is typical for many anhanguerians.

354 The sixth right alveolus is the largest, followed by the second, third, eighth and fourth,  
355 respectively, which are all subequal in size, and considerably larger than the first and seventh  
356 alveoli which are also comparable in size. The fifth right alveolus is the smallest rostrally and  
357 only slightly bigger than the more caudal eleventh and twelfth left alveoli, which are  
358 subequal in size (Table 1). Caudally, from the first alveolus, mesiodistal interalveolar  
359 distance increases gradually until the seventh alveolus. There is a significant increase in

360 interalveolar distance between the seventh and eight alveoli whereby the distance is almost  
361 double that of the preceding interalveolar measurement (Table 1).

362 *Comparisons:* The overall morphology and the extreme thinness of the cortical bone,  
363 measuring approximately 1.2 mm thick, identify KKF0600 as a pterosaur. The Lower  
364 Cretaceous age and, in part, large size (including a prominent premaxillary sagittal crest)  
365 indicate that the new specimen is referable to Pterodactyloidea. The strong resemblance of  
366 KKF0600 to the maxillary rostrum of several anhanguerids including, *Trop. mesembrinus*  
367 BSP 1987 I 46 (Wellnhofer, 1987), *F. lintoni* AODF 876 (Pentland et al., 2019) and  
368 *Anhanguera* spp. (e.g., Campos and Kellner, 1985, Veldmeijer, 2003, Kellner and Tomida,  
369 2000) verify the pterodactyloid pterosaur identification and its ornithocheiroid affinities. The  
370 presence of large rostral teeth rules out referral to the edentulous Cretaceous pterodactyloid  
371 clades Azhdarchidae, Tapejaridae, Pteranodontidae and Nyctosauridae. The dentition of  
372 KKF0600 also distinguishes it from Dsungaripteridae and Ctenochasmatidae; the former  
373 having edentulous jaw tips (e.g., Chen et al., 2020), the latter possessing extremely thin  
374 ‘needle-like’ teeth (e.g., Bennett, 2007).

375 Among Lanceodontia (*sensu* Holgado and Pêgas, 2020), the Australian specimen is distinct  
376 from Lower Cretaceous istiodactylid pterosaurs which are characterised by the possession of  
377 closely spaced, short triangular crowns occupied within a relatively broad, dorsoventrally  
378 flattened rostrum (e.g., Wang et al., 2008, Witton, 2012, Zhou et al., 2019). The lectotype of  
379 *Lonchodraco giganteus* (NHMUK PV 39412) possesses small alveoli (up to 6 alveoli per 30  
380 mm). *Lonchodraco giganteus* also possesses a deep palatal ridge. This differs considerably  
381 from the dental pattern seen in KKF0600. Furthermore, KKF660 lacks a palatal ridge.

382 *Hapterus gracilis* IVPP V11726 shares with KKF0600 (and most anhanguerians) strong and  
383 relatively large rostral teeth. However, the more caudal teeth of *H. gracilis* are characterized  
384 by a noticeable constriction at the base (Wang and Lü, 2001). Despite missing its tip, the

385 caudal tooth preserved on KKF0600 lacks any constriction at its base (Fig. 4A–D). Moreover,  
386 the rostrum of the Chinese taxon is pointed, contrasting with the more rounded and taller  
387 rostrum observed in KKF0600.

388 Boreopterid pterosaurs from the Lower Cretaceous Jehol Group of China are partly  
389 characterized by possessing a large number of teeth in both jaws, displaying two distinct  
390 morphologies: anteriormost teeth large and extremely thin; caudal teeth much shorter with a  
391 triangular outline (Lü and Ji, 2005, Lu, 2010, Jiang et al., 2014). The ‘needle-like’ rostral  
392 teeth of boreopterids are quite distinct, sharing more similarities with ctenochasmatids, and  
393 incongruent with the relatively large, oval-shaped rostral alveoli of KKF0600. Moreover, the  
394 caudal teeth of KKF0600, whilst smaller than the rostral teeth, are clearly not triangular.  
395 Boreopterids further differ from KKF0600 (and some targaryendraconians and  
396 anhanguerians) in lacking a dorsal deflection of the rostral tip.

397 In comparison with cimoliopterids, *Camposipterus nasutus* CAMSM B 54556, *Cimoliopterus*  
398 *cuvieri* NHMUK PV 39409 and *Cimoliopterus durni* SMU 76892 all share with KKF0600 a  
399 dorsally deflected rostral tip; the latter two taxa also possess similarly prominent, thin  
400 premaxillary crests with a concave rostral margin anteriorly (Rodrigues and Kellner, 2013,  
401 Myers, 2015). However, unlike KKF0600, the premaxillary crest of *Cim. cuvieri* and *Cim.*  
402 *durni* begins more caudally on the rostrum, above the seventh and fourth pair of alveoli,  
403 respectively. Cimoliopterids can be further differentiated from KKF0600 by possessing a  
404 palatal ridge, rostrally facing first tooth pair and an unusual dental pattern whereby the first  
405 three pairs of alveoli are positioned closely together (Pêgas et al., 2019). Finally, *Camp.*  
406 *nasutus* also has a dorsoventrally flattened rostrum (wider than high), which contrasts with  
407 the laterally compressed rostrum of KKF0600.

408 The Targaryendraconidae, comprising *Targaryendraco wiedenrothi* SMNS 56,628, *Aus.*  
409 *molnari* QM F10613 and *Barbosania gracilirostris* MHNS/00/85 are united on features  
410 relating only to the dentary (Pêgas et al., 2019). Only *B. gracilirostris* is represented by  
411 maxillary rostral material (Elgin and Frey, 2011), and shares with KKF0600 a dorsally  
412 deflected rostral tip, although the angle of deflection is slightly lower in the former taxon ( $10^\circ$   
413 compared with  $15^\circ$ ) and begins more caudally (dorsal to the tenth tooth position as opposed  
414 to the fourth). Comparable with KKF0600, the interalveolar distance in *B. gracilirostris*  
415 increases caudally (Elgin and Frey, 2011). However, it differs in having a crestless, pointed  
416 rostrum with the first pair of premaxillary teeth closely spaced together and positioned  
417 rostrorodorsally. Furthermore, from the first to the thirteenth tooth positions, the size of the  
418 alveoli remain constant in *B. gracilirostris*, differing from the pattern observed in KKF0600  
419 (and nearly all anhanguerians).

420 Hamipterids are primarily characterised by their well-developed premaxillary crests with  
421 well-defined parallel and rostrally curved striae and sulci (Holgado et al., 2019). In  
422 *Iberodactylus andreui* MPZ-2014/1 and all specimens of *Hamipterus tianshanensis*, the  
423 rostral margin of the crest begins noticeably caudal to the rostralmost margin of the rostrum  
424 (Wang et al., 2014, Holgado et al., 2019). This combination of features is not observed on  
425 the premaxillary crest of KKF0600. Furthermore, in hamipterids, the premaxillary tip is  
426 considerably laterally expanded (similar to the ‘spoon-shaped’ condition observed in  
427 anhanguerines), and a palatal ridge is present. These features also differ from KKF0600 and  
428 rules out referral to this clade.

429 As noted above, several aspects of the morphology of KKF0600, including the presence of a  
430 rounded, smooth and blade-like premaxillary crest and enlarged rostral teeth, are directly  
431 comparable with numerous anhanguerids. KKF0600 shares with *C. clavirostris* NHMUK PV  
432 R1822 and *Uktenadactylus rodriguesae* IWCMS 2014.82 several alveoli that are positioned

433 laterally on the rostrum (Owen, 1874, Holgado and Pêgas, 2020). However, in KKF0600, the  
434 eighth until the twelfth alveoli are positioned laterally, whilst in the aforementioned English  
435 coloborhynchines it is the second to the fourth alveoli. KKF0600 and coloborhynchines lack  
436 the prominent 'spoon-shaped' lateral expansion of the premaxillary tip that is seen in  
437 anhanguerines. However, the lateral expansion observed in KKF0600, albeit reduced in  
438 comparison with the condition seen in anhanguerines, is still rounded when viewed ventrally.  
439 This differs in coloborhynchines where the rostral lateral margins of the rostrum remain  
440 parallel, resulting in a quadrangular-shaped expansion when viewed ventrally. Moreover, in  
441 KKF0600, the first alveoli pair are positioned slightly caudal to the rostralmost margin of the  
442 rostrum, which is gently rounded in lateral view. This also differs in coloborhynchines where  
443 the first pair of alveoli are positioned on the flat, anteriormost palatal surface, which sharply  
444 rises dorsally from the ventral surface of the upper jaw.

445 Anhanguerinae (*sensu* Holgado et al., 2019) is a cosmopolitan clade of anhanguerid  
446 pterosaurs currently known from localities on four continents, including named species from  
447 the Santana Formation of Brazil (e.g., Campos and Kellner, 1985, Frey et al., 2003, Vila  
448 Nova et al., 2014), the Wessex Formation of England (Steel et al., 2005), the Ifezouane  
449 Formation (Kem Kem Group) of Africa (Smith et al., 2023) and the Jiufotang and Yixian  
450 formations of China (Wang and Zhou, 2003, Wang et al., 2012). Occurring from the  
451 Barremian through to the Albian, anhanguerines are supported by one synapomorphy: an  
452 enlarged fourth premaxillary tooth, larger than the fifth and sixth and as large as or larger  
453 than the third tooth (Holgado et al., 2019). Although no crown teeth are preserved on  
454 KKF0600, it clearly differs from the anhanguerine dental configuration by possessing an  
455 enlarged sixth alveolus that is slightly larger than second and third alveoli and larger than the  
456 fourth and fifth alveoli (Fig. 7). It also differs by possessing a smooth palatal surface, thus  
457 lacking a palatal ridge, a feature present in all anhanguerines. However, we do note that the

458 presence or absence of a palatal ridge is not observable in *Anhanguera piscator* as this region  
459 is concealed due to the closure of the jaws and the presence of matrix in the holotype (Kellner  
460 and Tomida, 2000). KKF0600 also lacks the prominent distal expansion of the rostral tip  
461 which is present in some anhanguerines (e.g., *Anhanguera* spp., *Maaradactylus kellneri*  
462 MPSC R 2357 and *Cearadactylus atrox* MN 7019-V) (Campos and Kellner, 1985, Kellner  
463 and Tomida, 2000, Bantim et al., 2014, Vila Nova et al., 2014).

464 Several morphological features of KKF0600 compare favourably with members of  
465 Tropeognathinae (*sensu* Holgado and Pêgas, 2020) (Fig. 8). A stratigraphically and  
466 geographically diverse clade, Tropeognathinae comprises *Tropeognathus mesembrinus* (BSP  
467 1987 I 46) from the Albian Romualdo Formation of Brazil (Wellnhofer, 1987), *Amblydectes*  
468 *crassidens* (CAMSM B54499) from the Cenomanian Cambridge Greensand of England  
469 (fossil-Albian in age) (Holgado, 2021), *Siroccoptyx moroccensis* (LINHM 016) from the  
470 Albian–lower Cenomanian Kem Kem beds of Morocco (Mader and Kellner, 1999) and three  
471 Australian taxa: *Thap. shawi* (Richards et al., 2021), and *M. camara* (Molnar and Thulborn,  
472 2007), both from the Albian Toolebuc Formation, and *F. lentoni* (AODF 876) from the upper  
473 Cenomanian–lower Turonian portion of the Winton Formation (Pentland et al., 2019).

474 The tropeognathine affinities of KKF0600 are well supported by the presence of a reduced  
475 premaxillary lateral expansion (under 130% post-rosette width; see Table 1) and a  
476 premaxillary crest that reaches the rostral tip. However, KKF0600 clearly differs from the  
477 non-Australian tropeognathines in terms of its alveolar morphology. In the latter taxa the first  
478 pair of alveoli are situated on the rostral-most surface of the rostrum (a condition similar to  
479 that observed in coloborhynchines), whereas in KKF0600 the first pair of alveoli are  
480 positioned slightly caudal to the rostral-most margin. Furthermore, in *Siroccoptyx*  
481 *moroccensis* the second to the eighth alveoli pairs are orientated ventrally, contrasting  
482 KKF0600 where the second to sixth alveoli are positioned lateroventrally, and the seventh

483 and eighth alveoli are positioned laterally on the rostrum. KKF0600 shares with *Amblydectes*  
484 *crassidens* in possessing a blunt rostralmost margin of the maxillary rostrum. However, in  
485 *Amblydectes crassidens*, despite lacking much of the left side, it is evident that the  
486 rostralmost margin is almost completely occupied by the first pair of alveoli (Holgado, 2021;  
487 fig.1, e and h). This differs considerably from KKF0600 where the rostralmost margin is  
488 noticeably taller (almost twice the height) and lacks alveoli.

489 Both *Siroccoptyx moroccensis* and *Trop. mesembrinus* possess a robust, well-defined 'keel-  
490 like' palatal ridge in the rostrum posterior to the fifth tooth, differing from KKF0600 where  
491 the corresponding portion of the palatal surface is relatively smooth and lacks a palatal ridge.  
492 As the holotype of *Amblydectes crassidens* preserves only the first three alveoli it is unknown  
493 if a palatal ridge was present caudal to this point. Finally, *Amblydectes crassidens*,  
494 *Siroccoptyx moroccensis* and *Trop. mesembrinus* lack robust, bony alveolar collars. This  
495 feature is only observed in the Australian tropeognathines.

496 Regarding the Australian tropeognathines, only *M. camara* and *F. lentoni* are represented by  
497 maxillary elements. The holotype of *Thap. shawi* comprises only the rostral portion of a  
498 mandible. Nevertheless, as previously noted, KKF0600 shares with all three Australian taxa  
499 robust bony alveolar collars. KKF0600 also shares with *F. lentoni* a large premaxillary crest  
500 with a tall rostral margin. The presence (or absence) of a premaxillary crest is unknown in *M.*  
501 *camara* and *Thap. shawi* given that in the former, the rostral portion of the skull is missing,  
502 and the latter preserves only the mandible. *Thap. shawi* does, however, possess a large  
503 mandibular crest and whilst this is by no means unequivocal proof for the existence of a  
504 premaxillary crest, we note that nearly all anhanguerids in possession of a mandibular crest  
505 also possess a premaxillary crest (e.g., Wellnhofer, 1987, Kellner and Tomida, 2000, Wang  
506 and Zhou, 2003, Pentland et al., 2019). The only exception being *Ludodactylus sibbicki*  
507 which possesses a low mandibular crest but lacks a premaxillary crest (Frey et al., 2003).

508 Therefore, it is not unreasonable to assume *Thap. shawi* most likely possessed a premaxillary  
509 crest; however, as there is no evidence of one in the holotype, this assumption remains  
510 speculative.

511 In lateral aspect, the rostral-most portion of the ventral surface of the palate is straight in *F.*  
512 *lentoni*, similar to *Trop. mesembrinus* and *Siroccoptyx moroccensis*. This differs from  
513 KKF0600 where the rostral-most portion of the palatal surface, starting immediately caudal  
514 to the fourth alveoli, is rostradorsally deflected at an angle of 15° relative to the caudal region  
515 of the palatal surface. This is remarkably similar to the condition seen in the mandible of  
516 *Thap. shawi* in which the rostralmost dorsal surface of the mandible is also rostradorsally  
517 deflected at an angle of 20°, starting near the fifth alveoli pair (Richards et al., 2021).

518 Unfortunately, the rostral-most portion of the maxilla is not preserved in *M. camara*.

519 Despite sharing robust alveolar collars, KKF0600 differs from *F. lentoni* in terms of alveolar  
520 configuration and spacing. In *F. lentoni*, the first pair of alveoli is positioned on the rostral-  
521 most margin of the premaxilla and orientated rostroventrally. The first alveolus is also  
522 smaller than all other rostrally positioned alveoli, a feature considered apomorphic by  
523 Pentland et al. (2019). In contrast, the first alveolus of KKF0600 is positioned rostrolaterally  
524 and orientated lateroventrally. In KKF0600, the fifth alveolus is the smallest, followed by the  
525 first and seventh alveoli, which are subequal in size. In *F. lentoni*, the remaining alveolar  
526 pairs, caudal to the first pair, are ventrally positioned and are orientated almost  
527 perpendicularly to the palatal surface, whereas in KKF0600 the remaining alveoli, caudal to  
528 the first alveolus, are positioned increasingly laterally on the upper jaw in a lateroventral  
529 orientation. From the rostral-most alveolar pair, interalveolar distance gradually increases  
530 caudally in *F. lentoni*, unlike KKF0600 where it increases caudally to the third alveoli, then  
531 decreases to the sixth before increasing again to the eighth alveoli. KKF0600 also differs

532 from *F. lentoni* in lacking a palatal ridge which in the latter initiates caudal to the second  
533 alveolar pair, becoming more prominent caudally (Pentland et al., 2019).

534 The holotype of *M. camara* preserves only the mid-section of the maxillary rostrum and  
535 corresponding mandibular region. As such, there is little anatomical overlap between the two  
536 specimens and comparisons with KKF0600 are therefore limited to the dentition and alveoli.  
537 Due to the preservation of *M. camara* it is unclear to which position the preserved alveoli  
538 correspond. However, given the rostralmost preserved teeth are positioned only slightly  
539 rostrally to the rostral margin of the nasoantorbital fenestra, it is presumed they represent  
540 alveoli caudal to the usually enlarged rostral teeth associated with the lateral expansion of the  
541 premaxillary tip, as seen in many anhanguerians (e.g., *Anhanguera* spp., *Trop. mesembrinus*  
542 and *Thap. shawi*). As such, the caudally positioned alveoli of *M. camara* are much larger than  
543 the caudal alveoli in KKF0600. The mesiodistal width of the eleventh and twelfth alveoli (8.7  
544 mm and 8.5 mm, respectively) preserved on KKF0600 are less than three quarters of the  
545 width of the rostralmost preserved tooth of *M. camara* (12.5 mm). Furthermore, in *M.*  
546 *camara*, the mesiodistal width of the rostralmost preserved tooth is larger than all but the  
547 sixth rostralmost alveoli preserved in KKF0600. Given that in most anhanguerians the rostral  
548 teeth were larger than the caudal teeth, it is likely that the overall dentition of *M. camara* was  
549 larger than that of KKF0600. In both taxa, the interalveolar distance of the caudal dentition  
550 decreases caudally, although in *M. camara* this distance is approximately twice as large. We  
551 do note however, that these size differences may be related to ontogenetic or dimorphic  
552 variation.

553 Whilst KKF0600 and *M. camara* share inflated bony alveoli collars, the rostralmost collar  
554 preserved on the maxilla of the latter is considerably taller, extending farther down the crown  
555 tooth, particularly on the mesial and distal edges. Caudal to the rostralmost preserved tooth in  
556 *M. camara*, the collars of the remaining alveoli are less robust and morphologically similar to

557 those observed in *Thap. shawi* and *F. lentoni*. However, the caudal alveolar collars in  
558 KKF0600 are positioned more laterally along the maxilla, presumably resulting in caudal  
559 teeth that are orientated lateroventrally, unlike *M. camara*, where the caudal maxillary alveoli  
560 are orientated ventrally. In a recent redescription of *M. camara*, Pentland and Poropat (2019)  
561 noted the presence of a row of several nutrient foramina in close proximity to several  
562 vascular channels positioned dorsal to the maxillary tooth row. While similar channels can be  
563 also be observed on the premaxillary crest of KKF0600 (Fig. 6), they are not associated with  
564 any nutrient foramina, which appear to be lacking in this taxon.

565 In terms of its alveolar morphology, KKF0600 is most similar to the configuration (alveolar  
566 size and interalveolar distance) observed on the mandible of the *Thap. shawi* holotype,  
567 KKF494. The graph of mesiodistal measurements of the alveoli (Fig. 7) show that in both  
568 specimens the third and sixth alveoli are the largest and slightly bigger than the second and  
569 fourth alveoli, which are comparable in size. The fifth alveolus is the smallest in both  
570 specimens. Caudally, in both specimens, the eleventh and twelfth alveoli are reduced in size  
571 and slightly smaller than the fifth. The graph of interalveolar distance (Fig. 7) shows a near  
572 identical trend in both specimens with a slight increase in distance caudally up to the fifth  
573 alveoli, followed by a marked increase between the fifth and sixth. Remarkably, in both  
574 specimens, the interalveolar distance between the seventh and eighth alveoli is almost double  
575 the length of the preceding interalveolar distance (between the sixth and seventh alveoli).

576 In KKF494, the first pair of alveoli are positioned slightly caudal to the rostralmost margin of  
577 the mandible and are orientated rostradorsally. The second to sixth alveolar pairs are  
578 positioned increasingly laterally on each dentary. Caudally, from the eighth alveolar pair, all  
579 alveoli are positioned on the lateral surface of the dentary. This arrangement is comparable  
580 with KKF0600 whereby the first alveoli pair are positioned slightly caudal to the  
581 premaxillary tip and orientated rostroventrally, the second alveoli pair are positioned

582 lateroventrally and, caudally, the remaining alveoli (third to twelfth pairs) are all positioned  
583 laterally on the maxillary rostrum.

584 As previously noted, the rostralmost ends of the respective maxillary and mandibular rostra  
585 of KKF0600 and the *Thap. shawi* holotype are deflected dorsally. Although the angle of  
586 deflection is slightly greater in *Thap. shawi* ( $20^\circ$  compared to  $15^\circ$ ), the point of deflection in  
587 both specimens initiates between the fourth and fifth alveoli. This feature presumably allows  
588 for tight occlusion between the upper and lower jaws and is often observed in anhanguerids  
589 where both the maxillary and mandibular rostra are preserved, e.g., *Anhanguera piscator*  
590 (Kellner and Tomida, 2000) and *Anhanguera spielbergi* (Veldmeijer, 2003). The exposed  
591 palatal surface of KKF0600 is relatively flat and lacks a palatal ridge. This feature (or lack  
592 thereof) complements the dorsal surface of the mandible in *Thap. shawi*, which, unlike other  
593 tropeognathines, is also flat and lacks a mandibular groove.

594 Given this suite of unique similarities, KKF0600 is herein referred to *Thapunngaka shawi*  
595 (Fig. 9). Despite the holotype of *Thap. shawi* (Richards et al., 2021) being represented by the  
596 rostral portion of a mandible, and thus sharing no anatomical overlap with KKF0600, this  
597 referral is based on both individuals sharing near identical features pertaining to alveolar  
598 morphology and patterning, and complementary similarities between the palatal and dentary  
599 occlusal surfaces, respectively.

## 600 **5. Phylogenetic analysis**

601 Using the modified character-taxon matrix of Richards et al. (2021), our phylogenetic  
602 analysis resulted in 18 most parsimonious trees, with 427 steps, a consistency index of 0.621,  
603 a retention index of 0.862 and a rescaled consistency index of 0.535. The strict consensus tree  
604 recovered *Thapunngaka shawi* within Tropeognathinae in a trichotomy containing *M.*  
605 *camara*, and *F. lentoni* (Figs. 10, S1). The placement of *Thapunngaka shawi* within

606 Tropeognathinae is supported by two unambiguous synapomorphies: premaxillary crest  
607 reaching the tip of the rostrum (Character 43, state 1), and a premaxillary expansion width  
608 less than 130% of the post-expansion width (Character 31, state 0). This clade, named here  
609 Mythungini is supported by one unambiguous synapomorphy: strongly raised alveoli borders  
610 (Character 129, present) and a bootstrap value of 50 (Fig. S2).

611 Our analysis also recovered Mythungini as the sister-group of *Tropeognathus mesembrinus* +  
612 *Siroccopteryx moroccensis* + *Amblydectes crassidens*. This latter clade, herein named  
613 Tropeognathini, is supported by two synapomorphies: wide and deep palatal ridge (Character  
614 75, state 2), that is restricted posteriorly to the fifth tooth position (Character 77, state 1).  
615 However, given the fragmentary nature of the holotype material, these synapomorphies  
616 cannot be assessed in *Amblydectes*, and its inclusion within Tropeognathini remains  
617 speculative until further material is described.

618 The remaining topology is in broad agreement with the phylogenies published by Holgado  
619 and Pêgas (2020) and Richards et al. (2021), the only exception being that *Caulkicephalus*  
620 *trimicrodon* + *Guidraco venator* were herein resolved as the sister group of *Ludodactylus*  
621 *sibbicki*.

## 622 **6. Discussion**

### 623 6.1 The new clade Mythungini

624 Nested within Tropeognathinae, the newly proposed clade Mythungini currently comprises  
625 the Australian anhanguerids *Mythunga camara*, *Ferrodraco lentoni* and *Thapunngaka shawi*  
626 (Fig. 10). Historically, our understanding of the relationships of Australian pterosaurs and  
627 exploration of their position within Pterosauria has been lacking. Until recently, phylogenetic  
628 analyses that included Australian pterosaur material were virtually absent from the literature.  
629 This exclusion was most likely due to the fragmentary nature of the fossils and the fact that

630 most of the Australian material represented isolated postcranial elements that were  
631 presumably regarded as phylogenetically uninformative.

632 Molnar and Thulborn (2007) originally regarded *M. camara* as an archaeoptero-  
633 (sensu Kellner, 2003). This assignment was based on a phylogenetic ‘assessment’, using  
634 selected cranial characters taken from the character-taxon matrices of Kellner (2003) and  
635 Unwin (2003). Although not a strict phylogenetic analysis per se, this study was ostensibly  
636 the first to explore the phylogenetic systematics of any Australian pterosaur. More recently, a  
637 detailed reassessment and subsequent reinterpretation of the holotype material of *M. camara*  
638 enabled Pentland and Poropat (2019) to re-evaluate the phylogenetic position of this taxon by  
639 its inclusion in a phylogenetic analysis for the first time. Using a data matrix modified from  
640 Andres et al. (2014), *M. camara* was recovered within Anhangueria, albeit in an unresolved  
641 position, supporting claims made previously by several workers regarding its anhanguerian,  
642 or anhanguerian-like affinities (e.g., Fletcher and Salisbury, 2010, Kellner et al., 2010,  
643 Kellner et al., 2011, Witton, 2013, Brougham et al., 2017).

644 Pentland et al. (2019) noted that *F. lentoni* shared with *M. camara* raised alveolar collars. In  
645 order to evaluate the phylogenetic position of *F. lentoni* they included both taxa in the data  
646 matrices modified from Andres et al. (2014) and Lü et al. (2018), recovering them as sister  
647 taxa within Anhangueria in the former analysis. Although raised alveolar borders were not  
648 explicitly scored for in the matrix modified from Andres et al. (2014), this relationship was  
649 supported by the presence of undulating lateral jaw margins (character 148, state 1). Holgado  
650 and Pêgas (2020), also recovered *M. camara* and *F. lentoni* in a sister-group relationship  
651 within the newly erected clade Tropeognathinae based on the shared synapomorphy of raised  
652 alveolar borders (character 129, present). Most recently, Richards et al. (2021) included  
653 *Thap. shawi* in two phylogenetic analyses based on the modified matrices of Holgado and  
654 Pêgas (2020) and Andres et al. (2014). The resulting topologies of both analyses recovered

655 *Thap. shawi*, *F. lentoni* and *M. camara* in an unresolved clade within Tropeognathinae and  
656 Ornithocheiridae, respectively.

657 In each of the aforementioned phylogenetic analyses, and the analysis presented herein,  
658 recovery of each clade containing the Australian anhanguerids (Mythungini) is based on the  
659 presence of one shared feature: strongly raised alveoli borders. Consequently, these alveoli  
660 borders give the lateral margins of the jaw a deeply undulated, or sulcate, appearance. This  
661 conspicuous feature was originally noted by Molnar and Thulborn (2007), describing *M.*  
662 *camara* as having a ‘strongly corrugated’ dentigerous margin of the jaw.

663 Whilst all ornithocheiraeans (with the exception of *Ornithocheirus simus*) have, at least to  
664 some extent, scalloped jaw margins, they are not as deeply sulcate between adjacent alveoli  
665 and, more significantly, they all lack strongly raised alveoli borders (e.g., Wellnhofer, 1987,  
666 Mader and Kellner, 1999, Pêgas et al., 2019). We note that while the holotype specimens of  
667 *Aetodactylus halli* (Myers, 2010) and *Unwindia trigonus* (Martill, 2011), and the lectotype  
668 specimen of *Lonchodraco giganteus* (Rodrigues and Kellner, 2013) also exhibit raised alveoli  
669 borders, they are significantly shorter and, consequently, much less prominent and entirely  
670 distinct to those seen in Mythungini. Furthermore, in *L. giganteus*, alveolar borders are  
671 present only on the rostral end of the upper and lower jaws (Rodrigues and Kellner, 2013).  
672 Contrastingly, in mythungins, this feature is observed along the entire jaw as preserved (for  
673 example, in *M. camara* they are present on the jaws caudal to rostralmost margin of the  
674 nasoantorbital fenestra).

675 Regarding the more inclusive clade Pterodactyloidea, we also note that ‘bulbously’ expanded  
676 alveolar protuberances are found on the jaws of certain dsungaripterids such as  
677 *Dsungaripterus weii* (Young, 1964), *Domeykodactylus ceciliae* (Martill et al., 2000),  
678 *Ordosipterus planignathus* (Ji, 2020) and, to a lesser degree, *Noriopterus complicidens*

679 (Young, 1973, Hone et al., 2017), however, this condition is vastly different in terms of both  
680 gross morphology and placement on the jaw and, consequently, quite distinct from the  
681 condition observed in the members of Mythungini. Similarly, the mandibular alveolar borders  
682 of *Pterodactylus sagittirostris* (NHMUK PV R 1823) were originally described as  
683 prominently rising “above the level of the surrounding part of the bone” (Owen, 1874).  
684 However, a redescription of the holotype by Rodrigues and Kellner (2013) revealed that the  
685 apparent elevation of the alveolar borders was an artifact of preparation, noting that the  
686 alveolar borders of the more extensively prepared right ramus were, in fact, smaller and  
687 similar to those found on other anhanguerids. Therefore, among ornithocheiraeans, and  
688 perhaps all lanceodontians (sensu Holgado and Pêgas, 2020), the possession of strongly  
689 raised alveolar borders is unique to Mythungini and herein considered a synapomorphy of the  
690 clade.

691 Given their spatiotemporal association with highly productive marine and lacustrine  
692 depositional environments and possession of a narrow, elongated rostrum with conical teeth,  
693 mythungins (like most ornithocheiraeans) are interpreted as piscivorous, possessing a diet  
694 consisting of fish and, possibly, other nektonic prey, all of which are well represented in the  
695 fossil record of areas in which they occurred. We propose that raised alveolar borders may  
696 have functioned as robust buttresses for each tooth, conferring some structural or mechanical  
697 advantage during foraging and/or feeding. This advantage may have consequently allowed  
698 mythungins to exploit more specialised, or access otherwise restricted dietary niches.  
699 However, we note that in order to satisfactorily test this hypothesis more material and  
700 subsequent functional morphological analyses are needed.

701 6.2 Another possible mythungin

702 A jaw fragment (WAM 68.5.11) recovered from the Cenomanian Molecap Greensand near  
703 Gingin in Western Australia preserves two adjacent alveoli from either the dentary or  
704 maxillary tooth rows (Kear et al., 2010:fig. 2A, C). The alveoli are labiolingually  
705 compressed, of different sizes, widely spaced (over four times the mesiodistal length of each  
706 alveolus) and are surrounded by raised alveolar borders or “flared alveolar rims” (Kear et al.,  
707 2010). Based on this limited suite of characters and its lower-Upper Cretaceous age the  
708 specimen was tentatively assigned to Ornithocheiridae (*sensu* Unwin, 2003). Kear et al.  
709 (2010) regarded WAM 68.5.11 to be most comparable to taxa such as *Anhanguera*,  
710 specifically ‘*Anhanguera*-like’ Australian taxa such as *M. camara*, *Aussiedraco molnari* and  
711 QMF44423 (a partial mandible assigned to Ornithocheiridae, gen. et sp. indet.) (Fletcher and  
712 Salisbury, 2010). This comparison was made on the basis that they all exhibit widely spaced,  
713 labiolingually compressed alveoli with raised alveolar borders. We agree that labiolingually  
714 compressed alveoli are present on all of the aforementioned Australian taxa and note that this  
715 feature is common among ornithocheiraeans (e.g., Kellner and Tomida, 2000, Holgado et al.,  
716 2019, Pêgas et al., 2019, Molnar and Thulborn, 2007). Widely spaced alveoli are also  
717 commonly found in anhanguerians (including *M. camara*, *F. lentoni* and *Thap. shawi*) but are  
718 not present in *Aussiedraco molnari* or QMF44423. Furthermore, while both *Aussiedraco*  
719 *molnari* and QMF44423 exhibit scalloped alveolar margins, they do not possess raised  
720 alveolar borders. In this feature, WAM 68.5.11 bears a closer resemblance to the alveolar  
721 morphology seen in mythungins and may represent a member of that clade. If so, an  
722 important paleobiogeographic inference may be drawn. The presence of *F. lentoni* and WAM  
723 68.5.11, in geographically disparate, yet contemporaneous, Upper Cretaceous sedimentary  
724 units would seemingly indicate that members of Mythungini were widespread across the  
725 entire continent during this period. However, given the extremely fragmentary nature of

726 WAM 68.5.11 and the subsequent lack of other discernible features, we presently regard its  
727 mythungin affinity and any consequent paleobiogeographic implication with caution.

### 728 6.3 Wingspan estimate of the new specimen of *Thapunngaka shawi* KKF600

729 For reasons outlined above, KKF600 is referred to *Thapunngaka shawi*. Importantly, this  
730 assignment represents the first record of Australian pterosaur material belonging to two  
731 distinct individuals of the same species. Although the rostrum of KKF600 is incomplete, a  
732 relative estimation of wingspan can be made by comparing KKF600 with the mandibular  
733 rostrum of the *Thapunngaka* holotype (KKF494). Based on the length of the mandibular  
734 symphysis, Richards et al. (2021) estimated the holotype to have a 6-7 m wingspan.

735 Comparatively, it is clearly evident that the new rostrum belongs to a slightly smaller  
736 individual with an estimated wingspan measuring 5-6 m. Although shorter than the wingspan  
737 of the *Thapunngaka shawi* holotype, it reinforces the idea that North West Queensland  
738 accommodated one of the largest species of anhanguerians known globally during the Early  
739 Cretaceous (Fig. 11).

## 740 7. Conclusions

741 The Australian pterosaur record has been repeatedly regarded as depauperate. Admittedly,  
742 when compared to pterosaur assemblages from South America, Europe and Asia, this view  
743 would seem to be justified. However, relatively recent discoveries of new taxa including at  
744 least four anhanguerians, a targaryendraconian, a ctenochasmatoïd and a putative azhdarchid  
745 suggests that the Australian pterosaur fauna was more diverse during the Cretaceous than  
746 previously thought. Representing a total of seven distinct taxa, the Australian pterosaur  
747 assemblage, whilst still undoubtedly underrepresented, is beginning to resemble the diversity  
748 seen in other assemblages such as from Morocco.

749

750 **Acknowledgments**

751 The authors sincerely thank R. Ievers, M. Johnston, K. Peterson and the staff at K.K. for access  
752 to the pterosaur material, including the *Thapunngaka shawi* holotype specimen. We also thank  
753 A. Rozefelds, S. Hocknull and K. Spring (Q.M.) for allowing T.M.R. access to the *Mythunga*  
754 *camara* and *Aussiedraco molnari* holotype specimens. P.E.S. and T.M.R would like to thank  
755 Gary and Barb Flewelling for assistance with the discovery of additional material at Cambridge  
756 Quarry. T.M.R. would like to personally thank J. Ristevski, A. Faith, B. Holland, A. Romilio,  
757 L. Leahey, J. Nair, A. Jannel and V. Weisbecker for lively discussions and useful suggestions.  
758 Special thanks to M. Anstis for providing information pertaining to Morungle Station. We are  
759 grateful to R. Molnar for providing unpublished material and support. The Willi Hennig  
760 Society is thanked for making TNT freely available. We express our gratitude to David Martill  
761 and an anonymous reviewer for their comments and suggestions that improved this manuscript.  
762 This research was supported by the Australian Government's Australian Biological Resources  
763 Study – National Taxonomy Research Grant Programme. We also acknowledge the people of  
764 the Wunumara Nation and their custodianship of the lands on which this specimen was found  
765 and pay our respects to their Ancestors and their descendants, who continue cultural and  
766 spiritual connections to Country. We recognise their valuable contributions to Australian and  
767 global society.

768

769 **REFERENCES**

770

- 771 ANDRES, B., CLARK, J. & XU, X. 2014. The Earliest pterodactyloid and the origin of the  
772 group. *Current Biology*, 24, 1011-1016.  
773  
774 BANTIM, R. A., SARAIVA, A. A., OLIVEIRA, G. R. & SAYAO, J. M. 2014. A new  
775 toothed pterosaur (Pterodactyloidea: Anhangueridae) from the Early Cretaceous  
776 Romualdo Formation, NE Brazil. *Zootaxa*, 3869, 201-223.  
777

- 778 BARRETT, P. M., BUTLER, R. J., EDWARDS, N. P. & MILNER, A. R. 2008. Pterosaur  
779 distribution in time and space: an atlas. *Zitteliana*, 61-107.  
780
- 781 BARTHOLOMAI, A. 2004. The large aspidorhynchid fish, *Richmondichthys sweeti*  
782 (Etheridge Jnr and Smith Woodward, 1891) from Albian marine deposits of  
783 Queensland, Australia. *Memoirs of the Queensland Museum*, 49, 521-536.  
784
- 785 BENNETT, S. C. 2002. Soft tissue preservation of the cranial crest of the pterosaur  
786 Germanodactylus from Solnhofen. *Journal of Vertebrate Paleontology*, 22, 43-48.  
787
- 788 BENNETT, S. C. 2007. A review of the pterosaur Ctenochasma: taxonomy and ontogeny.  
789 *Neues Jahrbuch für Geologie und Paläontologie-Abhandlungen*, 245, 23-31.  
790
- 791 BENNETT, S. C. & LONG, J. A. 1991. A large pterodactyloid pterosaur from the Late  
792 Cretaceous (Late Maastrichtian) of Western Australia. *Records of the Western*  
793 *Australian Museum*, 15, 435-443.  
794
- 795 BRALOWER, T. J., SLITER, W. V., ARTHUR, M. A., LECKIE, R. M., ALLARD, D. &  
796 SCHLANGER, S. O. 1993. Dysoxic/anoxic episodes in the Aptian-Albian (Early  
797 Cretaceous). *The Mesozoic Pacific: geology, tectonics, and volcanism*, 5-37.  
798
- 799 BROUGHAM, T., SMITH, E. T. & BELL, P. R. 2017. Isolated teeth of Anhangueria  
800 (Pterosauria: Pterodactyloidea) from the Lower Cretaceous of Lightning Ridge, New  
801 South Wales, Australia. *PeerJ*, 5, e3256.  
802
- 803 BURGER, D. 1982. Palynology of the Eromanga Basin and its applications. *Petroleum*  
804 *Exploration Society of Australia, Eromanga Basin Symposium*, 174.  
805
- 806 BUTLER, R. J., BENSON, R. B. & BARRETT, P. M. 2013. Pterosaur diversity: untangling  
807 the influence of sampling biases, Lagerstätten, and genuine biodiversity signals.  
808 *Palaeogeography, Palaeoclimatology, Palaeoecology*, 372, 78-87.  
809
- 810 CAMPBELL, R. & HAIG, D. 1999. Bathymetric change during Early Cretaceous  
811 intracratonic marine transgression across the northeastern Eromanga Basin, Australia.  
812 *Cretaceous Research*, 20, 403-446.  
813
- 814 CAMPOS, D. A. & KELLNER, A. W. A. 1985. Panorama of the flying reptiles study in  
815 Brazil and South America. *Anais da Academia Brasileira de Ciências*, 57, 453-466.  
816
- 817 CAVIN, L. & BERRELL, R. W. 2019. Revision of *Dugaldia emmilta* (Teleostei,  
818 Ichthyodectiformes) from the Toolebuc Formation, Albian of Australia, with  
819 comments on the jaw mechanics. *Journal of Vertebrate Paleontology*, 39, e1576049.  
820
- 821 CHEN, H., JIANG, S., KELLNER, A. W., CHENG, X., ZHANG, X., QIU, R., LI, Y. &  
822 WANG, X. 2020. New anatomical information on *Dsungaripterus weii* Young, 1964  
823 with focus on the palatal region. *Peer J*, 8, e8741.  
824
- 825 DAY, R. 1969. The Lower Cretaceous of the Great Artesian Basin. Australian National  
826 University Press, Canberra.  
827

- 828 ELGIN, R. A. & FREY, E. 2011. A new ornithocheirid, *Barbosania gracilirostris* gen. et sp.  
829 nov. (Pterosauria, Pterodactyloidea) from the Santana Formation (Cretaceous) of NE  
830 Brazil. *Swiss Journal of Palaeontology*, 130, 259.
- 831
- 832 EXON, N. F. & SENIOR, B. 1976. The Cretaceous of the Eromanga and Surat Basins. *BMR*  
833 *Journal of Australian Geology and Geophysics*, 1, 33-50.
- 834
- 835 FLETCHER, T. L. & SALISBURY, S. W. 2010. New pterosaur fossils from the Early  
836 Cretaceous (Albian) of Queensland, Australia. *Journal of Vertebrate Paleontology*,  
837 30, 1747-1759.
- 838
- 839 FREY, E., MARTILL, D. M. & BUCHY, M.-C. 2003. A new crested ornithocheirid from the  
840 Lower Cretaceous of northeastern Brazil and the unusual death of an unusual  
841 pterosaur. *Geological Society, London, Special Publications*, 217, 55-63.
- 842
- 843 GOLOBOFF, P. A. & CATALANO, S. A. 2016. TNT version 1.5, including a full  
844 implementation of phylogenetic morphometrics. *Cladistics*, 32, 221-238.
- 845
- 846 GRAY, A., MCKILLOP, M., MCKELLAR, J. & DRAPER, J. 2002. Eromanga basin  
847 stratigraphy. *Geology of the Cooper Eromanga Basins, Queensland*, 1, 30-56.
- 848
- 849 HENDERSON, R. & KENNEDY, W. 2002. Occurrence of the ammonite *Goodhallites*  
850 *goodhalli* (J. Sowerby) in the Eromanga Basin, Queensland: an index species for the  
851 late Albian (Cretaceous). *Alcheringa*, 26, 233-247.
- 852
- 853 HOLGADO, B. 2021. On the validity of the genus *Amblydectes* Hooley 1914  
854 (Pterodactyloidea, Anhangueridae) and the presence of Tropeognathinae in the  
855 Cambridge Greensand. *Anais da Academia Brasileira de Ciências*, 93.
- 856
- 857 HOLGADO, B. & PÊGAS, R. V. 2020. A taxonomic and phylogenetic review of the  
858 anhanguerid pterosaur group Coloborhynchinae and the new clade Tropeognathinae.  
859 *Acta Palaeontologica Polonica*, 65, 743-761.
- 860
- 861 HOLGADO, B., PÊGAS, R. V., CANUDO, J. I., FORTUNY, J., RODRIGUES, T.,  
862 COMPANY, J. & KELLNER, A. W. 2019. On a new crested pterodactyloid from the  
863 Early Cretaceous of the Iberian Peninsula and the radiation of the clade Anhangueria.  
864 *Scientific reports*, 9, 1-10.
- 865
- 866 HONE, D., XU, X. & JIANG, S. 2017. A taxonomic revision of *Noriopteris complicidens*  
867 (Young, 1973) and Asian members of Dsungaripteridae. *Geological Society, London,*  
868 *Special Publications*, 455, 149-157.
- 869
- 870 JACOBS, M. L., MARTILL, D. M., IBRAHIM, N. & LONGRICH, N. 2019. A new species  
871 of *Coloborhynchus* (Pterosauria, Ornithocheiridae) from the mid-Cretaceous of North  
872 Africa. *Cretaceous Research*, 95, 77-88.
- 873
- 874
- 875 JELL, P. A. 2013. *Geology of Queensland*, Geological Survey of Queensland.
- 876

- 877 JI, S.-A. 2020. First record of Early Cretaceous pterosaur from the Ordos Region, Inner  
878 Mongolia, China. *China Geology*, 3, 1-7.  
879
- 880 JIANG, K., LIN, C., ZHANG, X., HE, W. & XIAO, F. 2018. Geochemical characteristics  
881 and possible origin of shale gas in the Toolebuc Formation in the Northeastern part of  
882 the Eromanga Basin, Australia. *Journal of Natural Gas Science and Engineering*.  
883
- 884 JIANG, S.-X., WANG, X.-L., MENG, X. & CHENG, X. 2014. A new boreopterid pterosaur  
885 from the Lower Cretaceous of western Liaoning, China, with a reassessment of the  
886 phylogenetic relationships of the Boreopteridae. *Journal of Paleontology*, 88, 823-  
887 828.  
888
- 889 KAUP, J. 1834. Versuch einer Eintheilung der Säugethiere in 6 Stämme und der Amphibien  
890 in 6 Ordnungen. *Isis*, 3, 311-315.  
891
- 892 KEAR, B. P. 2006. First gut contents in a Cretaceous sea turtle. *Biology letters*, 2, 113-115.  
893
- 894 KEAR, B. P. 2007a. First record of a pachycormid fish (Actinopterygii: Pachycormiformes)  
895 from the Lower Cretaceous of Australia. *Journal of Vertebrate Paleontology*, 27,  
896 1033-1038.  
897
- 898 KEAR, B. P. 2007b. Taxonomic clarification of the Australian elasmosaurid genus  
899 *Eromangasaurus*, with reference to other austral elasmosaur taxa. *Journal of*  
900 *Vertebrate Paleontology*, 27, 241-246.  
901
- 902 KEAR, B. P., DEACON, G. L. & SIVERSON, M. 2010. Remains of a Late Cretaceous  
903 pterosaur from the Molecap Greensand of Western Australia. *Alcheringa*, 34, 273-  
904 279.  
905
- 906 KELLNER, A. W. 2003. Pterosaur phylogeny and comments on the evolutionary history of  
907 the group. *Geological Society, London, Special Publications*, 217, 105-137.  
908
- 909 KELLNER, A. W. & CAMPOS, D. A. 2002. The function of the cranial crest and jaws of a  
910 unique pterosaur from the Early Cretaceous of Brazil. *Science*, 297, 389-392.  
911
- 912 KELLNER, A. W., CAMPOS, D. A., SAYAO, J. M., SARAIVA, A. A., RODRIGUES, T.,  
913 OLIVEIRA, G., CRUZ, L. A., COSTA, F. R., SILVA, H. P. & FERREIRA, J. S.  
914 2013. The largest flying reptile from Gondwana: a new specimen of *Tropeognathus*  
915 cf. *T. mesembrinus* Wellnhofer, 1987 (Pterodactyloidea, Anhangueridae) and other  
916 large pterosaurs from the Romualdo Formation, Lower Cretaceous, Brazil. *Anais da*  
917 *Academia Brasileira de Ciências*, 85, 113-135.  
918
- 919 KELLNER, A. W., RICH, T. H., COSTA, F. R., VICKERS-RICH, P., KEAR, B. P.,  
920 WALTERS, M. & KOOL, L. 2010. New isolated pterodactyloid bones from the  
921 Albian Toolebuc Formation (western Queensland, Australia) with comments on the  
922 Australian pterosaur fauna. *Alcheringa*, 34, 219-230.  
923
- 924 KELLNER, A. W., RODRIGUES, T. & COSTA, F. R. 2011. Short note on a pteranodontoid  
925 pterosaur (Pterodactyloidea) from western Queensland, Australia. *Anais da Academia*  
926 *Brasileira de Ciências*, 83, 301-308.

- 927  
928 KELLNER, A. W., RODRIGUES, T., COSTA, F. R., WEINSCHUTZ, L. C., FIGUEIREDO,  
929 R. G., SOUZA, G. A., BRUM, A. S., ELEUTERIO, L. H., MUELLER, C. W. &  
930 SAYAO, J. M. J. 2019. Pterodactyloid pterosaur bones from Cretaceous deposits of  
931 the Antarctic Peninsula. *Anais da Academia Brasileira de Ciências*, 91.  
932
- 933 KELLNER, A. W. A. & TOMIDA, Y. 2000. Description of a new species of Anhangueridae  
934 (Pterodactyloidea) : with comments on the pterosaur fauna from the Santana  
935 Formation (Aptian-Albian), northeastern Brazil *National Science Museum*  
936 *Monographs*, 17, ix-137.  
937
- 938 KUROCHKIN, E. N. & MOLNAR, R. E. 1997. New material of enantiornithine birds from  
939 the Early Cretaceous of Australia. *Alcheringa: An Australasian Journal of*  
940 *Palaeontology*, 21, 291-297.  
941
- 942 LEAHEY, L. G. & SALISBURY, S. W. 2013. First evidence of ankylosaurian dinosaurs  
943 (Ornithischia: Thyreophora) from the mid-Cretaceous (late Albian–Cenomanian)  
944 Winton Formation of Queensland, Australia. *Alcheringa: An Australasian Journal of*  
945 *Palaeontology*, 37, 249-257.  
946
- 947 LEES, T. & BARTHOLOMAI, A. 1987. Study of a Lower Cretaceous actinopterygian (Class  
948 Pisces) *Cooyoo australis* from Queensland, Australia. *Memoirs of the Queensland*  
949 *Museum*, 25, 177-192.  
950
- 951 LONGMAN 1915. On a giant turtle from the Queensland Lower Cretaceous. *Memoirs of the*  
952 *Queensland Museum*, 3, 24-29.  
953
- 954 LU, J. 2010. A new boreopterid pterodactyloid pterosaur from the Early Cretaceous Yixian  
955 Formation of Liaoning Province, northeastern China. *Acta Geologica Sinica - English*  
956 *Edition*, 84, 241-246.  
957
- 958 LÜ, J. & JI, Q. 2005. A new ornithocheirid from the Early Cretaceous of Liaoning Province,  
959 China. *Acta Geologica Sinica - English Edition*, 79, 157-163.  
960
- 961 LÜ, J., MENG, Q., WANG, B., LIU, D., SHEN, C. & ZHANG, Y. 2018. Short note on a new  
962 anurognathid pterosaur with evidence of perching behaviour from Jianchang of  
963 Liaoning Province, China. In: HONE, D. W. E., WITTON, M. P. & MARTILL, D.  
964 M. (eds.) *New Perspectives on Pterosaur Palaeobiology*. *Geological Society, London,*  
965 *Special Publications*. London: The Geological Society of London.  
966
- 967 MADER, B. J. & KELLNER, A. W. A. 1999. A new anhanguerid pterosaur from the  
968 Cretaceous of Morocco. *Museo Nacional. Nova Serie, Geologia*, 45, 1-11.  
969
- 970 MARTILL, D. M. 2011. A new pterodactyloid pterosaur from the Santana Formation  
971 (Cretaceous) of Brazil. *Cretaceous Research*, 32, 236-243.  
972
- 973 MARTILL, D. M., FREY, E., DIAZ, G. C. & BELL, C. 2000. Reinterpretation of a Chilean  
974 pterosaur and the occurrence of Dsungaripteridae in South America. *Geological*  
975 *Magazine*, 137, 19-25.  
976

- 977 MCHENRY, C. R. 2009. *'Devourer of Gods': The palaeoecology of the Cretaceous pliosaur*  
978 *Kronosaurus queenslandicus*. PhD thesis, University of Newcastle.  
979
- 980 MCMINN, A. & BURGER, D. 1986. Palynology and palaeoenvironment of the Toolebuc  
981 Formation (sensu lato) in the Eromanga Basin. *Contributions to the geology and*  
982 *hydrocarbon potential of the Eromanga Basin. Geological Society of Australia,*  
983 *Special Publication, 12, 139-154.*  
984
- 985 MOLNAR, R. 1987. A pterosaur pelvis from western Queensland, Australia. *Alcheringa, 11,*  
986 *87-94.*  
987
- 988 MOLNAR, R. 1996. Observations on the Australian ornithopod dinosaur *Muttaborrasaurus*.  
989 *Memoirs of the Queensland Museum, 39, 639-652.*  
990
- 991 MOLNAR, R. E. 1986. An enantiornithine bird from the Lower Cretaceous of Queensland,  
992 Australia. *Nature, 322, 736-738.*  
993
- 994 MOLNAR, R. E. 1991. *Fossil reptiles in Australia*, Melbourne, Australia, Monash University  
995 Publications Committee.  
996
- 997 MOLNAR, R. E. & SALISBURY, S. W. 2005. Observations on Cretaceous sauropods from  
998 Australia. In: TIDWELL, V. & CARPENTER, K. (eds.) *Thunder-lizards: the*  
999 *sauropodomorph dinosaurs*. Bloomington, Indiana: Indiana University Press.  
1000
- 1001 MOLNAR, R. E. & THULBORN, R. A. 1980. First pterosaur from Australia. *Nature, 288,*  
1002 *361-363.*  
1003
- 1004 MOLNAR, R. E. & THULBORN, R. A. 2007. An incomplete pterosaur skull from the  
1005 Cretaceous of north-central Queensland, Australia. *Arquivos do Museu Nacional, Rio*  
1006 *de Janeiro, 65, 461-470.*  
1007
- 1008 MYERS, T. S. 2010. A new ornithocheirid pterosaur from the Upper Cretaceous  
1009 (Cenomanian–Turonian) Eagle Ford Group of Texas. *Journal of Vertebrate*  
1010 *Paleontology, 30, 280-287.*  
1011
- 1012 MYERS, T. S. 2015. First North American occurrence of the toothed pteranodontoid  
1013 pterosaur *Cimoliopterus*. *Journal of Vertebrate Paleontology, 35, e1014904.*  
1014
- 1015 OWEN, R. 1874. Monograph on the fossil Reptilia of the Mesozoic formations.  
1016 *Palaeontographical Society, London, 14.*  
1017
- 1018 OWEN, R. 1882. On an extinct chelonian reptile (*Notochelys costata*, Owen), from Australia.  
1019 *Quarterly Journal of the Geological Society, 38, 178-183.*  
1020
- 1021 PÊGAS, R. V., HOLGADO, B. & LEAL, M. E. C. 2019. On *Targaryendraco wiedenrothi*  
1022 gen. nov. (Pterodactyloidea, Pteranodontoidea, Lanceodontia) and recognition of a  
1023 new cosmopolitan lineage of Cretaceous toothed pterodactyloids. *Historical Biology,*  
1024 *1-15.*  
1025

- 1026 PENTLAND, A. H. & POROPAT, S. F. 2019. Reappraisal of *Mythunga camara* Molnar &  
1027 Thulborn, 2007 (Pterosauria, Pterodactyloidea, Anhangueria) from the upper Albian  
1028 Toolebuc Formation of Queensland, Australia. *Cretaceous Research*, 93, 151-169.  
1029
- 1030 PENTLAND, A. H., POROPAT, S. F., TISCHLER, T. R., SLOAN, T., ELLIOTT, R. A.,  
1031 ELLIOTT, H. A., ELLIOTT, J. A. & ELLIOTT, D. A. 2019. *Ferrodraco lentoni* gen.  
1032 et sp. nov., a new ornithocheirid pterosaur from the Winton Formation (Cenomanian–  
1033 lower Turonian) of Queensland, Australia. *Scientific Reports*, 9, 1-13.  
1034
- 1035 PLIENINGER, F. 1901. Beiträge zur Kenntniss der Flugsaurier. *Palaeontographica*, 48, 65-  
1036 90.  
1037
- 1038 POROPAT, S. F., NAIR, J. P., SYME, C. E., MANNION, P. D., UPCHURCH, P.,  
1039 HOCKNULL, S. A., COOK, A. G., TISCHLER, T. R. & HOLLAND, T. 2017.  
1040 Reappraisal of *Austrosaurus mckillopi* Longman, 1933 from the Allaru Mudstone of  
1041 Queensland, Australia's first named Cretaceous sauropod dinosaur. *Alcheringa: An  
1042 Australasian Journal of Palaeontology*, 41, 543-580.  
1043
- 1044 RICHARDS, T. M., STUMKAT, P. E. & SALISBURY, S. W. 2021. A new species of  
1045 crested pterosaur (Pterodactyloidea, Anhangueridae) from the Lower Cretaceous  
1046 (upper Albian) of Richmond, North West Queensland, Australia. *Journal of  
1047 Vertebrate Paleontology*, e1946068.  
1048
- 1049 RODRIGUES, T. & KELLNER, A. W. A. 2013. Taxonomic review of the *Ornithocheirus*  
1050 complex (Pterosauria) from the Cretaceous of England. *ZooKeys*, 1-112.  
1051
- 1052 SEELEY, H. G. 1870. *The Ornithosauria: An elementary study of the bones of pterodactyls,*  
1053 *made from fossil remains found in the Cambridge Upper Greensand, and arranged in*  
1054 *the Woodwardian Museum of the University of Cambridge*, Cambridge, Deighton,  
1055 Bell & Co.  
1056
- 1057 SENIOR, B., EXON, N. & BURGER, D. 1975. The Cadna-owie and Toolebuc formations in  
1058 the Eromanga Basin, Queensland. *Queensland Government Mining Journal*, 76, 445-  
1059 455.  
1060
- 1061 SMITH, R. E., IBRAHIM, N., LONGRICH, N., UNWIN, D. M., JACOBS, M. L.,  
1062 WILLIAMS, C. J., ZOUHRI, S. & MARTILL, D. M. 2023. The pterosaurs of the  
1063 Cretaceous Kem Kem Group of Morocco. *PalZ*, 97, 519-568.  
1064
- 1065 STEEL, L., MARTILL, D. M., UNWIN, D. M. & WINCH, J. D. 2005. A new pterodactyloid  
1066 pterosaur from the Wessex Formation (Lower Cretaceous) of the Isle of Wight,  
1067 England. *Cretaceous Research*, 26, 686-698.  
1068
- 1069 SYME, C. E., WELSH, K. J., ROBERTS, E. M., & SALISBURY, S. W. 2016. Depositional  
1070 environment of the Lower Cretaceous (Upper Albion) Winton Formation at Isisford,  
1071 Central-West Queensland, Australia, inferred from sandstone concretions. *Journal of  
1072 Sedimentary Research*, 86, 1067-1082.  
1073

- 1074 TUCKER, R. T., ROBERTS, E. M., HU, Y., KEMP, A. I. & SALISBURY, S. W. 2013.  
1075 Detrital zircon age constraints for the Winton Formation, Queensland: contextualizing  
1076 Australia's Late Cretaceous dinosaur faunas. *Gondwana Research*, 24, 767-779.  
1077
- 1078 UNWIN, D. M. 2003. On the phylogeny and evolutionary history of pterosaurs. *Geological*  
1079 *Society, London, Special Publications*, 217, 139-190.  
1080
- 1081 UNWIN, D. M. 2006. *The Pterosaurs From Deep Time*, New York, New York, Pi Press.  
1082
- 1083 VELDMEIJER, A. J. 2003. Description of *Coloborhynchus spielbergi* sp.  
1084 nov.(Pterodactyloidea) from the Albian (Lower Cretaceous) of Brazil. *Scripta*  
1085 *Geologica*, 125, 35-139.  
1086
- 1087 VELDMEIJER, A. J. 2006. Toothed pterosaurs from the Santana Formation (Cretaceous;  
1088 Aptian—Aptian) of northeastern Brazil. A reappraisal on the basis of newly described  
1089 material. PhD thesis, Utrecht University.  
1090
- 1091 VILA NOVA, B. C., SAYÃO, J. M., NEUMANN, V. H. M. L. & KELLNER, A. W. A.  
1092 2014. Redescription of *Cearadactylus atrox* (Pterosauria, Pterodactyloidea) from the  
1093 Early Cretaceous Romualdo Formation (Santana Group) of the Araripe Basin, Brazil.  
1094 *Journal of Vertebrate Paleontology*, 34, 126-134.  
1095
- 1096 WANG, X.-L. & ZHOU, Z.-H. 2003. Two new pterodactyloid pterosaurs from the Early  
1097 Cretaceous Jiufotang Formation of western Liaoning, China. *Vertebrata Palasiatica*,  
1098 41, 34-49.  
1099
- 1100 WANG, X., CAMPOS, D. A., ZHOU, Z. & KELLNER, A. W. A. 2008. A primitive  
1101 istiodactylid pterosaur (Pterodactyloidea) from the Jiufotang Formation (Early  
1102 Cretaceous), northeast China. *Zootaxa*, 1813, 1 - 18.  
1103
- 1104 WANG, X., KELLNER, A. W., JIANG, S., WANG, Q., MA, Y., PAIDOUOLA, Y., CHENG,  
1105 X., RODRIGUES, T., MENG, X., ZHANG, J., LI, N. & ZHOU, Z. 2014. Sexually  
1106 dimorphic tridimensionally preserved pterosaurs and their eggs from China. *Current*  
1107 *Biology*, 24, 1323-1330.  
1108
- 1109 WANG, X., KELLNER, A. W. A., JIANG, S. & CHENG, X. 2012. New toothed flying  
1110 reptile from Asia: close similarities between early Cretaceous pterosaur faunas from  
1111 China and Brazil. *Naturwissenschaften*, 99, 249-257.  
1112
- 1113 WANG, X. & LÜ, J. 2001. Discovery of a pterodactylid pterosaur from the Yixian Formation  
1114 of western Liaoning, China. *Chinese Science Bulletin*, 46, 1112-1117.  
1115
- 1116 WELLNHOFER, P. J. 1987. New crested pterosaurs from the Lower Cretaceous of Brazil.  
1117 *Mitteilungen der Bayerischen Staatssammlung für Paläontologie und historische*  
1118 *Geologie*, 27, 175-186.  
1119
- 1120 WITTON, M. P. 2012. New insights into the skull of *Istiodactylus latidens*  
1121 (Ornithocheiroidea, Pterodactyloidea). *PLoS One*, 7, e33170.  
1122

- 1123 WITTON, M. P. 2013. *Pterosaurs: natural history, evolution, anatomy*, Princeton University  
1124 Press.  
1125
- 1126 XIAOLIN, W. & ZHONGHE, Z. 2006. Pterosaur assemblages of the Jehol Biota and their  
1127 implication for the Early Cretaceous pterosaur radiation. *Geological Journal*, 41, 405-  
1128 418.  
1129
- 1130 YOUNG, C. C. 1964. On a new pterosaurian from Sinkiang, China. *Vertebrata palasiatica*,  
1131 8, 221.  
1132
- 1133 YOUNG, C. C. 1973. Reports of paleontological expedition to Sinkiang (II). Pterosaurian  
1134 fauna from Wuerho, Sinkiang. *Memoirs of the Institute of Vertebrate Palaeontology  
1135 and Paleoanthropology, Academy Sinica*, 11, 18-35.  
1136
- 1137 ZAMMIT, M. 2010. A review of Australasian ichthyosaurs. *Alcheringa: An Australasian  
1138 Journal of Palaeontology*, 34, 281-292.  
1139
- 1140 ZHOU, X., PÊGAS, R. V., LEAL, M. E. & BONDE, N. 2019. *Nurhachius luei*, a new  
1141 istiodactylid pterosaur (Pterosauria, Pterodactyloidea) from the Early Cretaceous  
1142 Jiufotang Formation of Chaoyang City, Liaoning Province (China) and comments on  
1143 the Istiodactylidae. *Peer J*, 7, e7688.

1144

1145

1146

## FIGURE CAPTIONS

1147 FIGURE 1. Geological map of the Richmond area of North West Queensland, showing the  
1148 locations (red triangles) where pterosaur specimens have been found. **1**, KKF0600 [this  
1149 study]; **2**, *Thapunngaka shawi*, KKF494; **3**, *Mythunga camara*, QM F18896). Geological  
1150 outcrop data for the Rolling Downs Group modified from Richards et al. (2021). Scale bar  
1151 equals 10 km. [planned for full page width]

1152

1153 FIGURE 2. Stratigraphy of the Eromanga Basin, North West Queensland (after Syme et al.,  
1154 2016) with a partial view of the type locality of KKF0600 at the Cambridge Downs site.  
1155 Dashed line indicates the bedding horizon where KKF0600 was located. Scale bar equals 1  
1156 m. [planned for full page width]

1157

1158 FIGURE 3. KKF0600, the rostral portion of a pterosaur rostrum from the upper Albian  
 1159 Toolebuc Formation, Wunumara Country, near Richmond, north-west Queensland, Australia.  
 1160 Photo and schematic interpretation in: **A** and **B**, right lateral view; **C** and **D**, ventral view; **E**  
 1161 and **F**, rostral view. Darker shading in **B** indicates a natural mould of the left lateral surface of  
 1162 the rostrum on the matrix. Cranial direction is indicated by an arrow in **A–D**, and numbers  
 1163 correspond to alveolar positions. **Abbreviations:** **bc**, broken crown; **l#**, left; **og**, occlusal  
 1164 groove; **pmc**, premaxillary crest; **r#**, right. Scale bar equals 25 mm. [planned for full page  
 1165 width]

1166

1167 FIGURE 4. Detailed view of smaller fragment of KKF0600, a portion of the left maxilla and  
 1168 palatal surface. Photo and schematic interpretation in: **A** and **C**, left lateral view; **B** and **D**,  
 1169 ventral view; **E** and **F**, ventrolateral view showing position on larger fragment. Hatched  
 1170 shading in **C**, **D** and **F** indicates surface breaks. Cranial is indicated by an arrow in **D** and **F**,  
 1171 and numbers correspond to inferred alveolar positions. **Abbreviations:** **bc**, broken crown.  
 1172 Scale bars in **A–D** and **E–F** equal 10 mm. [planned for full page width]

1173

1174 FIGURE 5. Members of Mythungini clade nov., and detailed views of their raised alveolar  
 1175 collars, respectively. **A**, *Thapunngaka shawi* Richards, Stumkat and Salisbury, (present  
 1176 study), KKF0600, Richmond, Queensland, Australia, upper Albian, Toolebuc Formation, in  
 1177 right lateral and **B**, ventral views. **C**, *Thapunngaka shawi* Richards, Stumkat and Salisbury,  
 1178 2021, KKF494, Richmond, Queensland, Australia, upper Albian, Toolebuc Formation, in  
 1179 right lateral and **D**, ventral views. **E** and **F**, *Ferrodraco lentoni* Pentland, Poropat, Tischler,  
 1180 Sloan, Elliot, 2019, AODF 876, Winton, Queensland, Australia, upper Cenomanian–lower  
 1181 Turonian, Winton Formation, in left lateral views. **G** and **H**, *Mythunga camara* Molnar and

1182 Thulborn, 2007, QM F18896, Hughenden, Queensland, Australia, Albian, Toolebuc  
1183 Formation, in left lateral views. **E** and **F** modified from Pentland et al. (2019) under a CC-BY  
1184 4.0 license. All other photographs taken by TMR. Scale bar equals 50 mm. [planned for full  
1185 page width]

1186

1187 FIGURE 6. Partial rostrum of *Thapunngaka shawi* (KKF0600) in right lateral view. White  
1188 arrows indicate channels interpreted as possible blood vessels. Black arrows indicate ridges  
1189 present in the matrix resulting from the natural moulding of channels present on the left  
1190 lateral side of the rostrum. Scale bar equals 10 mm. [planned for full page width]

1191

1192 FIGURE 7. The dentition pattern of various anhanguerids showing: **A**, the size of mesiodistal  
1193 alveolar length; Y-axis equals natural log-transformed length, X-axis refers to alveolus  
1194 position. **B**, the size of inter-alveolar distance; Y-axis equals natural log-transformed  
1195 distance, X-axis refers to alveolus position. Measurements of *Tropeognathus mesembrinus*,  
1196 *Anhanguera blittersdorffi* and *Anhanguera araripensis* taken from Veldmeijer (2006). All  
1197 other measurements were taken from first-hand study of the specimens. [planned for full page  
1198 width]

1199

1200 FIGURE 8. Tropeognathinae rostra comparative plate. **A**, *Amblydectes crassidens* in (**A1**)  
1201 rostral and (**A2**) ventral views; **B**, *Siroccopteryx moroccensis* in (**B1**) rostral and (**B2**) ventral  
1202 views; **C**, *Tropeognathus mesembrinus* in (**C1**) rostral and (**C2**) ventral views; **D**, *Ferrodraco*  
1203 *lentoni* in (**D1**) rostral and (**D2**) ventral views; **E**, *Thapunngaka shawi* in (**E1**) rostral and (**E2**)  
1204 ventral view. Dashed line indicates surface breaks or extent of specimen shown. Cranial  
1205 direction is indicated by an arrow in **A2–E2** and numbers correspond to tooth and/or alveolar

1206 positions. Black area in **D<sub>2</sub>** indicates position of lower tooth **Abbreviations: bc**, broken  
1207 crown; **mdc**, dentary crest; **pmc**, premaxillary crest; **prid**, palatal ridge. Scale bar equals 50  
1208 mm. Drawings by TMR based on Holgado and Pêgas (2020). [planned for full page width]

1209

1210 FIGURE 9. Hypothetical reconstruction of the skull of *Thapunngaka shawi*. Scale bar equals  
1211 100 mm. [planned for 1.5 column width]

1212

1213 FIGURE 10. Time-calibrated phylogenetic tree showing the relationship of *Thapunngaka*  
1214 *shawi* within Lanceodontia. Taxon ranges, denoted by the box adjacent to each taxon, include  
1215 both the true stratigraphic range and uncertainty, whereas the colour of the box reflects the  
1216 paleocontinental origin of each taxon. Hatched box shows uncertain temporal range. Based  
1217 on the data matrix of Holgado and Pêgas (2020), with characters of *Thapunngaka shawi*  
1218 scored from both the referred specimen (KKF600) and the holotype (KKF494) included. New  
1219 clades and taxon proposed in this paper marked in bold. [planned for full page width]

1220

1221 FIGURE 11. Life restoration of *Thapunngaka shawi*. Image copyright James Kuether.  
1222 [planned for full page width]

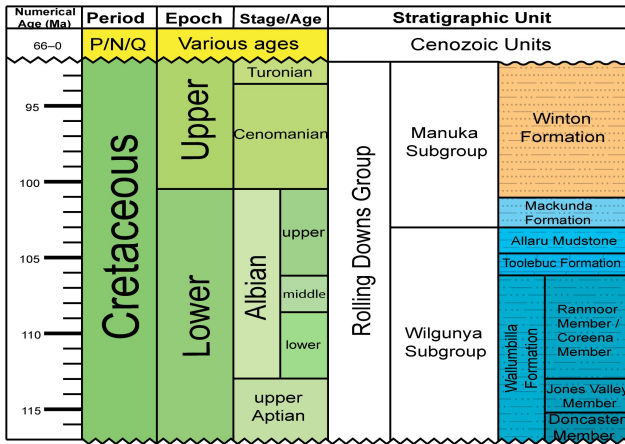
**TABLE 1.** Measurements of KKF0600, *Thapunngaka shawi*, from the Toolebuc Formation of North West Queensland, Australia.

KKF0600 large fragment measurements	(mm)
Length as preserved–right premaxilla/maxilla	312
Height as preserved–premaxillary crest	82.8
Length as preserved–premaxillary crest	240
Width of premaxillary crest at broken dorsal margin	2.9
Exposed width of palate at:	
1 <sup>st</sup> alveolus	11.5
2 <sup>nd</sup> alveolus	10.3
3 <sup>rd</sup> alveolus	10.6
4 <sup>th</sup> alveolus	9.5
5 <sup>th</sup> alveolus	7.6
6 <sup>th</sup> alveolus	8.1
7 <sup>th</sup> alveolus	7.2
8 <sup>th</sup> alveolus	6.8
Right alveoli (mesiodistal length):	
1	9.8
2	11.7
3	11.3
4	10.3
5	9.1*
6	12.9*
7	9.8

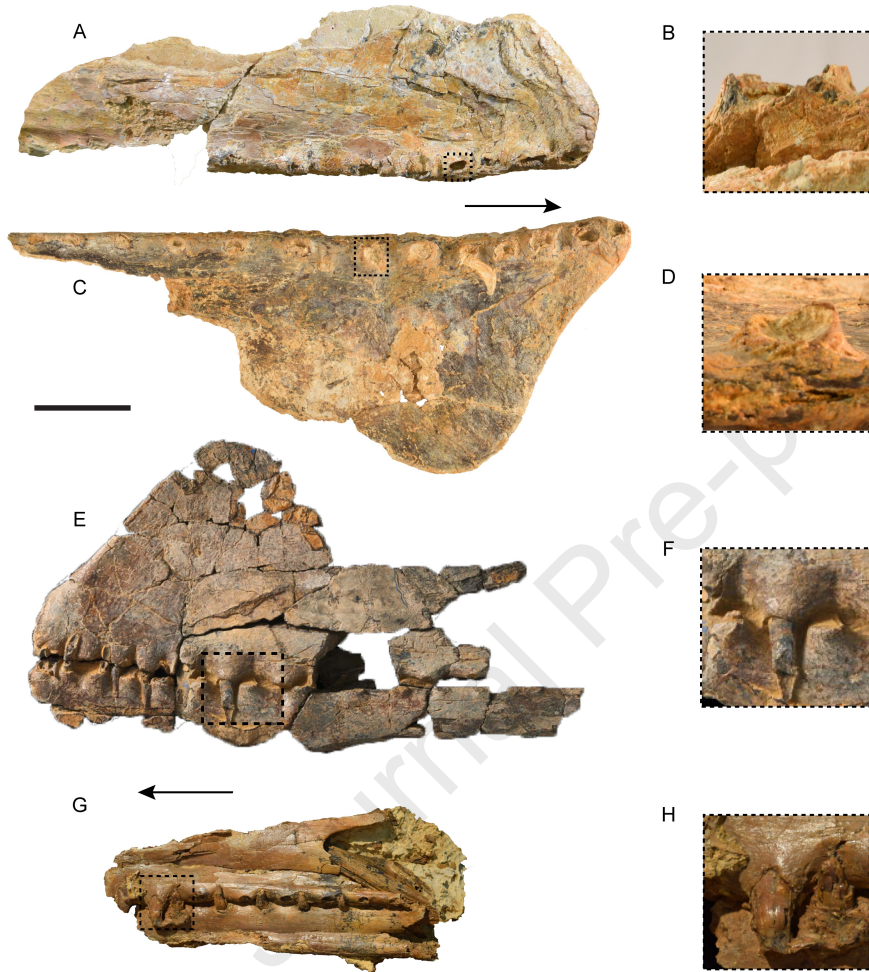
**TABLE 1.** (continued)

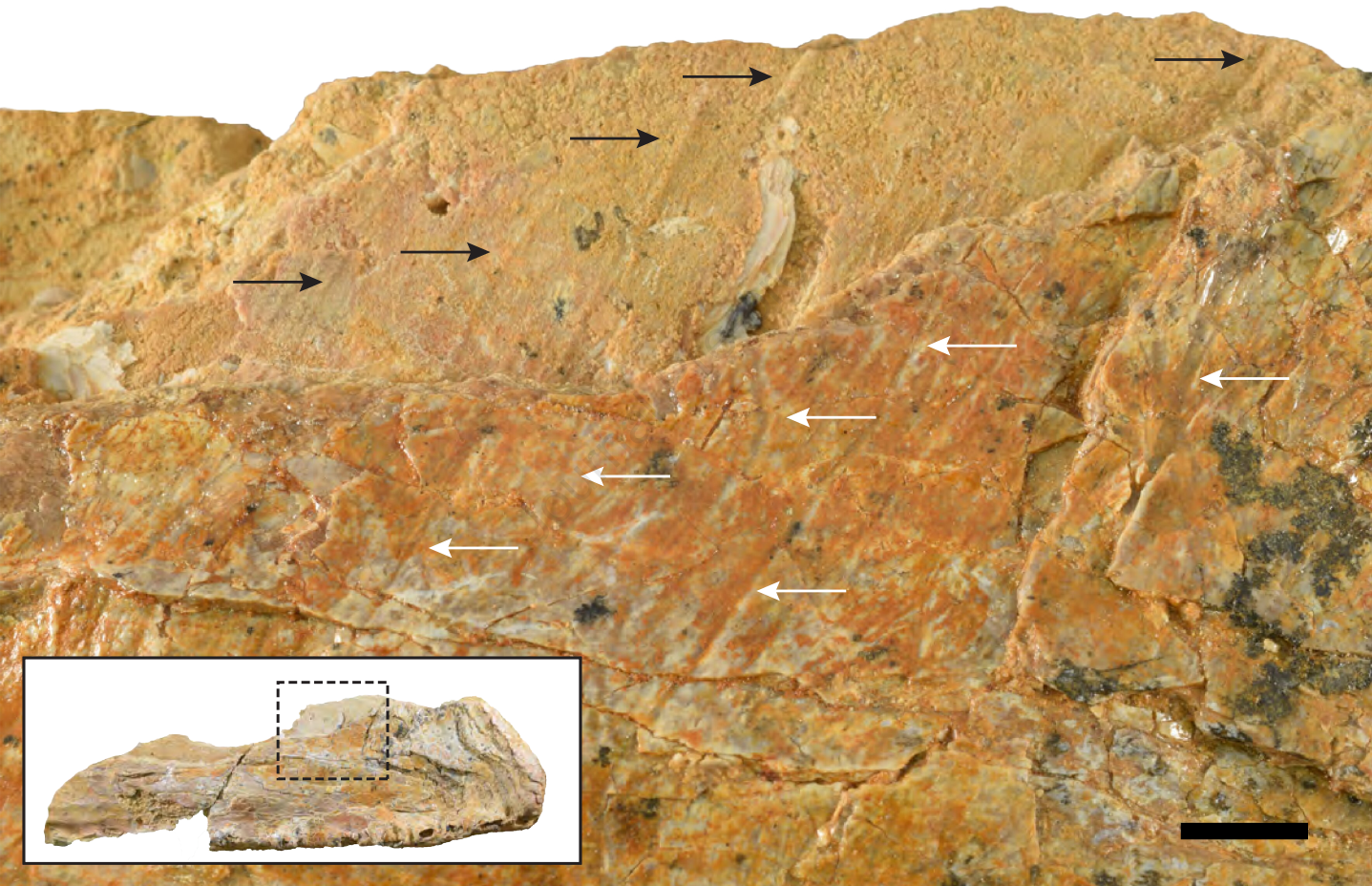
8	10.4*
Left alveoli–mesiodistal length as preserved	
6	5.3 <sup>†</sup>
Interalveolar distance between:	
1–2	6.4
2–3	7.8
3–4	7.7
4–5	7.4
5–6	11.0
6–7	13.5
7–8	23.7
<hr/>	
KKF0600 smaller posterior fragment measurements	(mm)
<hr/>	
Length as preserved–palate	34.7
Width as preserved–palate	12.5
Left alveoli (mesiodistal length):	
11	8.7
12	8.5
Interalveolar distance between:	
11–12	12.7
Height as preserved–tooth crown in 12 <sup>th</sup> alveolus	9.7
<hr/>	

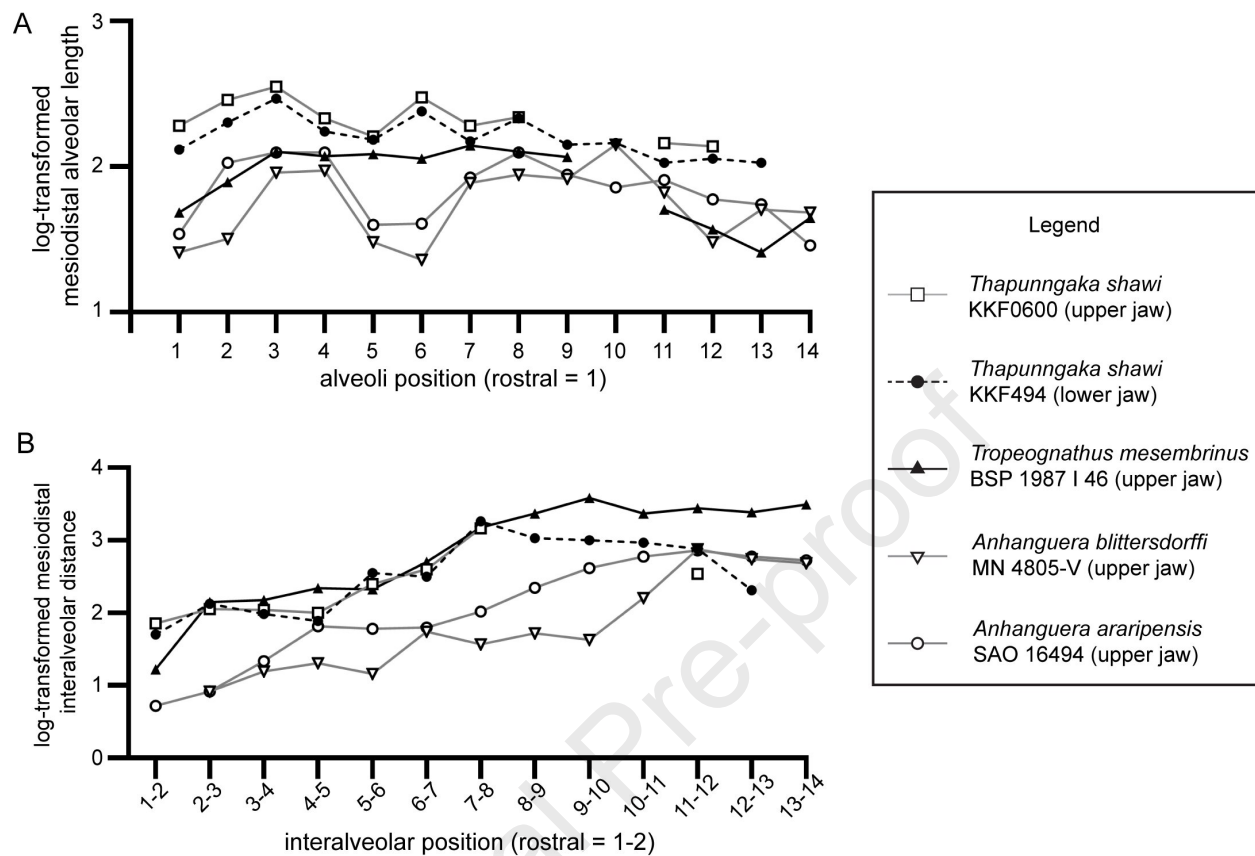
\*: approximate, <sup>†</sup>: partially embedded in matrix

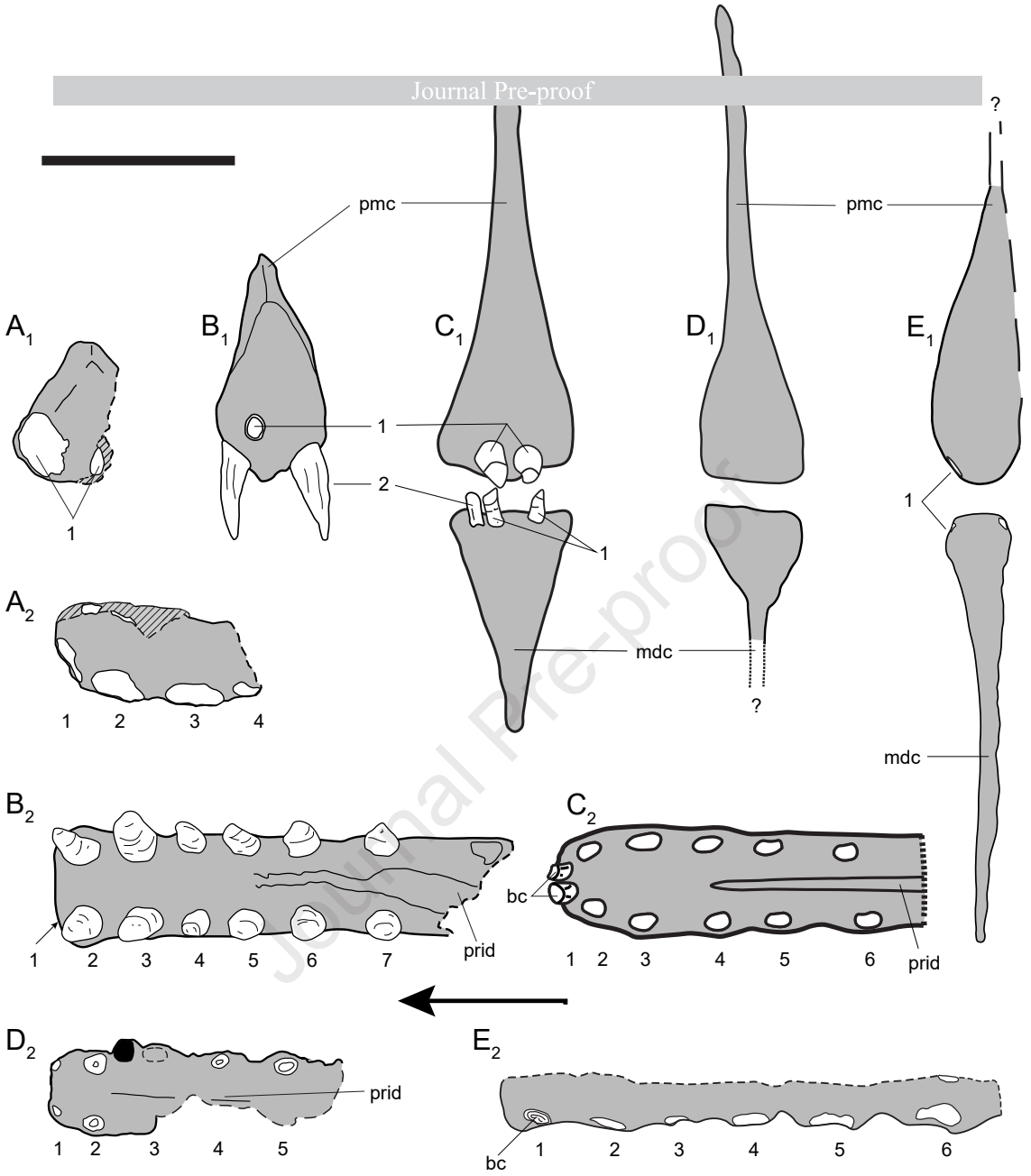


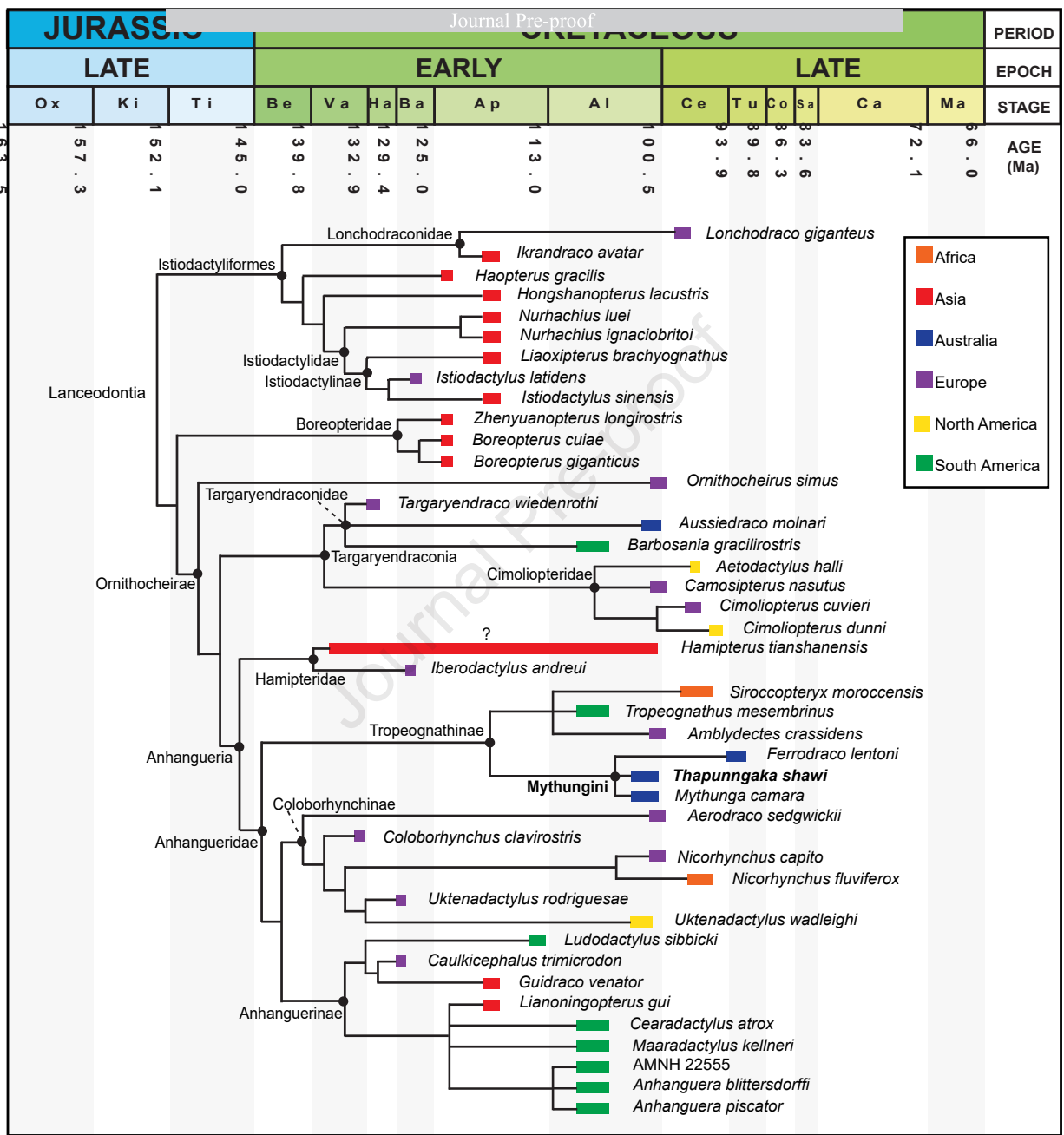
Journal Pre-proof

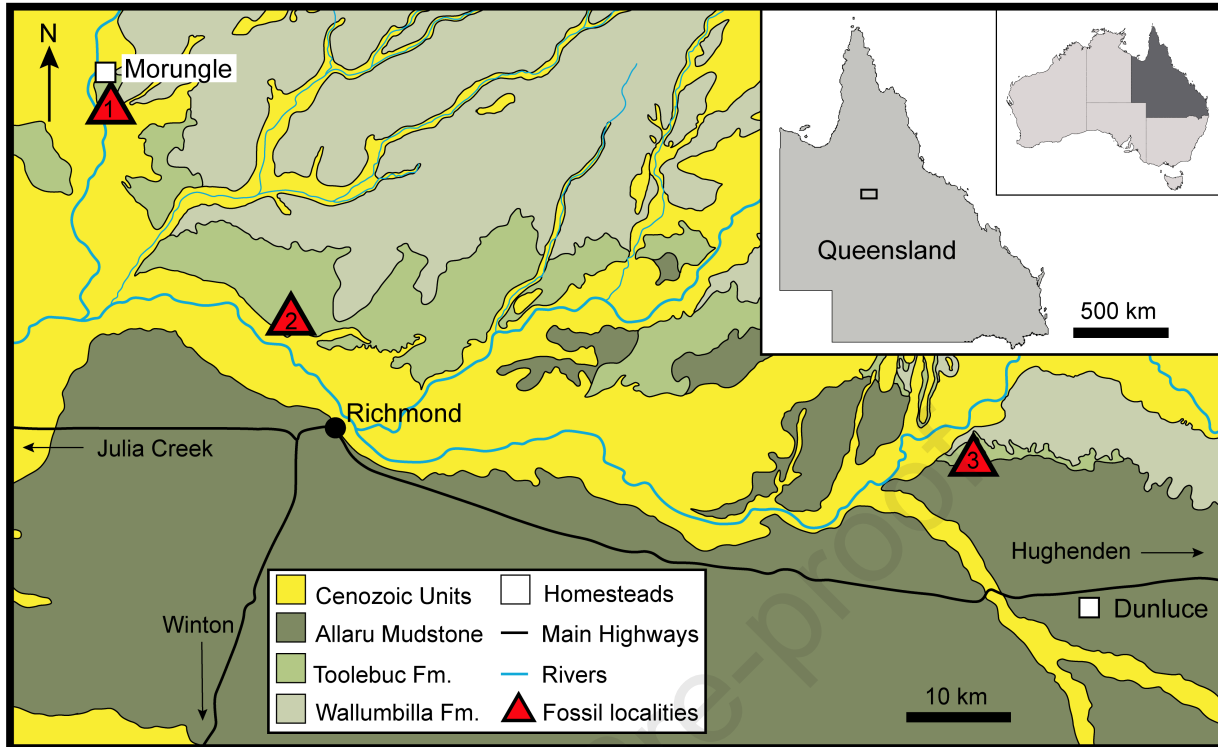


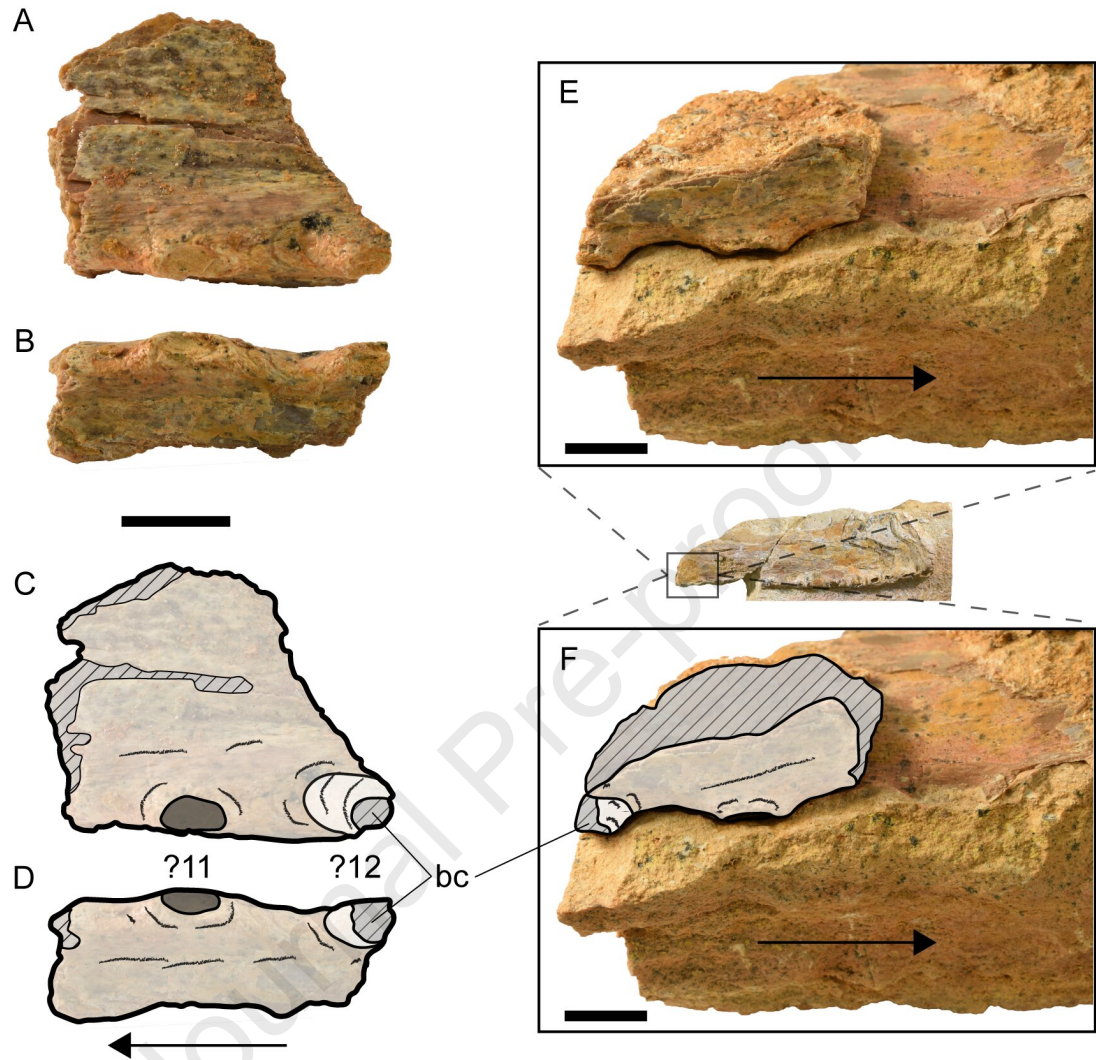


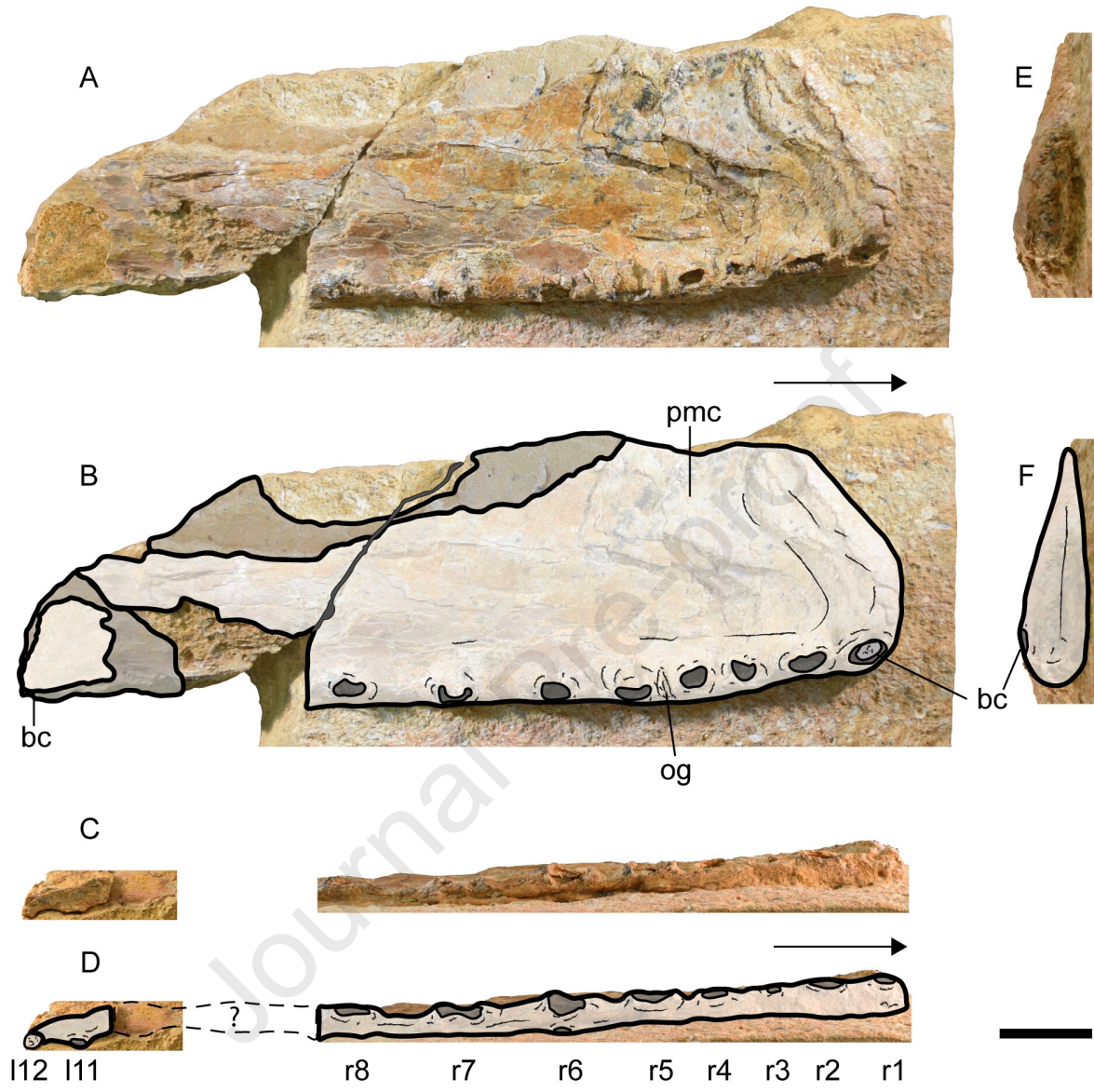


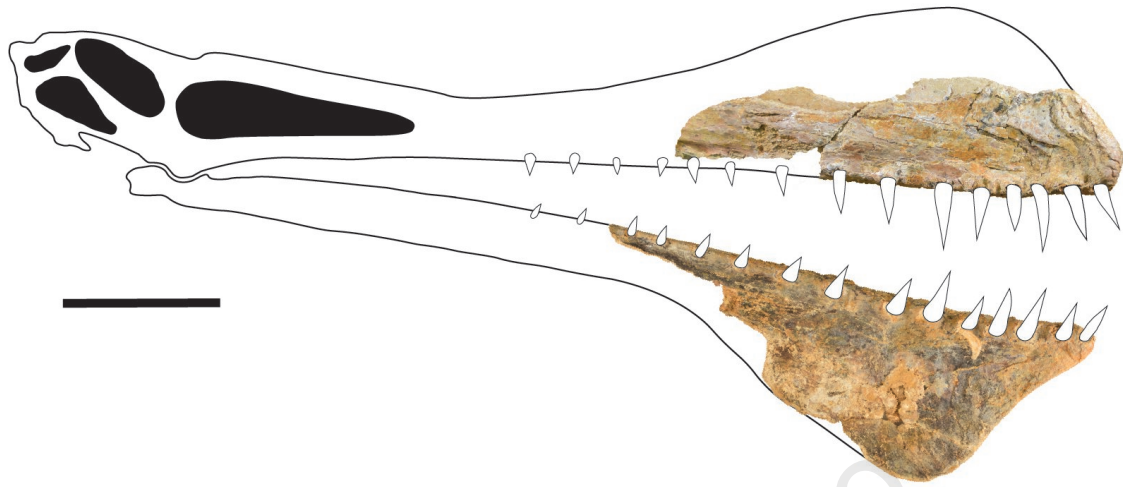














Journal

## Highlights

- A second specimen of *Thapunngaka shawi*, a large anhanguerid pterosaur from the Lower Cretaceous (upper Albian) Toolebuc Formation of North West Queensland, Australia is described.
- A revised diagnosis of *Thapunngaka shawi* is presented.
- Phylogenetic analysis recovers a new clade formed by *Thapunngaka shawi*, *Ferrodraco lentoni* and *Mythunga camara*.
- The recognition of this new East Gondwanan pterosaur clade, Mythungini, points to a possible endemic radiation within Tropeognathinae.
- This is the first report of a second specimen belonging to an Australian pterosaur species.

**Declaration of interests**

The authors declare that they have no known competing financial interests or personal relationships that could have appeared to influence the work reported in this paper.

The authors declare the following financial interests/personal relationships which may be considered as potential competing interests:

Journal Pre-proof

Credit author statement

**Timothy Richards:** Conceptualization, Methodology, Investigation, Software, Visualization, Writing-Original draft preparation **Paul Stumkat:** Investigation, Writing- Reviewing and Editing **Steven Salisbury:** Supervision, Writing- Reviewing and Editing.

Journal Pre-proof